J. Comp. Path. 2011, Vol. 144, 204–211

Available online at www.sciencedirect.com

ScienceDirect

ELSEVIER
www.elsevier.com/locate/jcpa

SHORT PAPER

Periventricular Leucomalacia (PVL)-like Lesions in Two Neonatal Cynomolgus Monkeys (*Macaca fascicularis*)

S. Okabayashi*,†, K. Uchida‡, H. Nakayama‡, C. Ohno*, K. Hanari*, I. Goto* and Y. Yasutomi†

** Corporation for Production and Research of Laboratory Primates, Hachimandai 1-1, Tsukuba-shi, Ibaraki 305-0843, † Tsukuba Primate Research Center, National Institute of Biomedical Innovation, Hachimandai 1-1, Tsukuba-shi, Ibaraki 305-0843 and ‡ Laboratory of Veterinary Pathology, Graduate School of Agricultural and Life Sciences, The University of Tokyo, Yayoi 1-1-1, Bunkyo-ku, Tokyo 113-8657, Japan*

Summary

Periventricular leucomalacia (PVL) is a lesion of immature cerebral white matter that occurs in the perinatal period. In man, PVL is the predominant form of brain injury and a cause of cerebral palsy and cognitive deficits in premature infants. PVL affects fetuses and newborns, particularly those who have undergone oxygen deprivation as may occur in premature birth. Many clinical and pathological studies of PVL have been performed in man, but there is no clear definition of PVL in animals. A few spontaneous PVL-like cases in puppies or experimental cases in other animal species have been reported. The present study reports the histopathological and immunohistochemical features of PVL-like lesions in two neonatal cynomolgus monkeys. In both cases, there was cerebral white matter necrosis with marked infiltration of lipid-laden phagocytes and a reduction of neurons in the cerebral cortex. In case 1 there was extensive cavitation of the cerebral white matter. In case 2 there was reactive astrocytosis associated with a decrease in oligodendroglial cells and a decrease in cerebral white matter myelin. To our knowledge, this is the first report of PVL-like leucoencephalomalacia in non-human primates.

Keywords: cynomolgus monkey; histopathology; immunohistochemistry; periventricular leucomalacia

Cerebral white matter injury in premature human infants is a problem of major clinical importance. These injuries take the form of multiple different lesions including intraventricular haemorrhage, post-haemorrhagic hydrocephalus and periventricular leucomalacia (PVL). PVL is the major form of cerebral white matter injury that affects premature infants and is associated with the subsequent development of cerebral palsy. The characteristic lesion of PVL consists of focal periventricular necrosis, with subsequent cyst formation and more diffuse cerebral white matter injury (Khwaja and Volpe, 2008). Although the pathogenesis of PVL remains to be completely elucidated, it is likely that the necrosis of white matter relates to impaired perfusion resulting from hypoxia–ischaemia (Khwaja and Volpe, 2008). An alternative hypothesis proposes that the lesions result from intrauterine infection with direct toxic effects on fetal oligodendrocytes and astrocytes by cytokines (Damman and Levinton, 1997). Risk factors for PVL include prematurity, asphyxia, respiratory distress, septicaemia, chorioamnionitis, arterial hypotension and hypocarbia (Resch *et al.*, 2004).

There is no clear definition of PVL in animals; however, animal models are necessary for understanding the mechanism of PVL in man. Although a few spontaneous PVL-like cases have been described in puppies (Rentmeister *et al.*, 2004) and several experimental cases (Young *et al.*, 1982; Levison *et al.*, 2001; Brazel *et al.*, 2004) have been reported, no model

Correspondence to: S. Okabayashi (e-mail: okarin@primate.or.jp).

0021-9975/$ - see front matter
doi:10.1016/j.jcpa.2010.06.006

reliably replicates all aspects of human PVL. Non-human primates have motor functions and cognitive abilities similar to man and have therefore become increasingly important as experimental models for the study of human central nervous system (CNS) disease. However, PVL-like disease has yet to be described in non-human primates. Here, we report two spontaneously arising cases of PVL-like lesions in neonatal cynomolgus monkeys (*Macaca fascicularis*).

Case 1 was a neonatal female cynomolgus monkey from the Tsukuba Primate Research Center (TPRC) that was delivered by caesarean section at 163 days of gestation as the mother had difficulties in parturition associated with profuse vaginal haemorrhage. The neonate did not breathe for several minutes, but was successfully resuscitated. The body weight of the monkey was 290 g and the animal was artificially nursed. Three days later, paralysis of the limbs was observed and the monkey became progressively debilitated due to insufficient sucking of milk. Despite treatment with subcutaneous infusion of 5% glucose solution and emergency medical care, the monkey died naturally 21 days after birth.

Case 2 was a neonatal male cynomolgus monkey born in the TPRC 16 days prior to the expected date of confinement. The mother rejected the neonate and artificial nursing was conducted. Despite the preterm birth, the body weight of this monkey was 290 g (the average weight of neonatal cynomolgus monkeys in the TPRC is approximately 300–350 g). The next day, paralysis of the limbs was observed and the monkey could not suck sufficient milk. Because this monkey had abnormal breath sounds 3 days after birth, the veterinarian continued treatment with subcutaneous infusion of 5% glucose solution and antibiotics. However, the monkey died naturally 7 days after birth.

Necropsy examination was performed in each case. Tissues were fixed in 10% neutral buffered formalin, processed routinely and embedded in paraffin wax. Sections (3 μm) were stained with haematoxylin and eosin (HE). For immunohistochemistry (IHC), dewaxed sections were pretreated with H_2O_2 0.5% in methanol and then subjected to antigen retrieval by immersion in citric acid buffer (pH 6.0) and heating in an autoclave for 10 min at 121°C. Sections were then incubated free floating in primary antibody solution overnight at 4°C. Primary antibodies were mouse monoclonal antibodies specific for glial fibrillary acidic protein (GFAP, clone LF2, Dako, Glostrup, Denmark; 1 in 200 dilution), CD68 (clone KP1, Dako; 1 in 100 dilution), vimentin (clone 3B4, Dako; 1 in 200 dilution), neurofilament (NF, clone 2F11, Dako; 1 in 100 dilution) and active-caspase-3 (Cas3; Chemicon, Temecula, California; 1 in 100 dilution). Following brief washes with buffer, the sections were incubated sequentially with polymer immunocomplex (Dako) for 30 min. Immunoreactive elements were 'visualized' by treating the sections with 3, 3′-diaminobenzidine tetroxide (Dojin Kagaku, Kunamoto, Japan) followed by counterstaining with haematoxylin.

For double immunolabelling, sections were dewaxed and then stained with 1% Sudan black B to reduce autofluorescence. Following brief washes, sections were incubated free floating overnight at 4°C in solutions containing mouse monoclonal antibody for myelin basic protein (MBP; Chemicon; 1 in 500 dilution) and rabbit polyclonal antibody specific for oligodendrocytes (olig2; IBL, Takasaki, Gunma, Japan; 1 in 500 dilution). Sections were then incubated with AlexaFluor 488-conjugated goat anti-mouse IgG (Invitrogen, Carlsbad, California; 1 in 1,000 dilution) and AlexaFluor 555-conjugated goat anti-rabbit IgG (Invitrogen; 1 in 1,000 dilution) for 1 h at room temperature. The sections were examined with a Digital Eclipse C1 confocal microscope (Nikon, Kanagawa, Japan). Neonatal monkey brain sections (0-day-old animals) were used as normal controls.

Grossly, the neonatal monkeys were emaciated, dehydrated and had pale mucous membranes. Both limbs and the tail had a decreased range of motion and atrophy of limb muscles was observed in each case. Both tracheas were filled with mucus mixed with milk. The lungs were oedematous and hyperaemic and there were several small white nodules (2–3 mm diameter) in all pulmonary lobes in case 2. In case 1, an excessive quantity of cerebrospinal fluid (CSF) had accumulated in the cranial cavity and the volume of the cerebrum appeared reduced. After formalin fixation, cross sections of the cerebrum in case 1 revealed the presence of marked cavitation of the white matter and atrophy of the cortical region (Fig. 1A), whereas multiple foci of softening of the white matter were found in cross sections of the cerebrum in case 2 (Fig. 1B).

Microscopically, in case 1 areas of cavitation or foci of liquefactive necrosis were widespread with loss of all cellular elements from white matter to deep gray matter, with many lipid-filled phagocytes aggregated within the necrotic foci (Fig. 2A). Residual cerebral cortex showed marked reduction in the number of neural cells. The lateral ventricle was enlarged, with hyperaemia of the choroid plexus, and the ependymal layers showed glial cell infiltration and partial exfoliation. Glial cell infiltration, glial nodules and aggregation of lipid-filled phagocytes with formation of cholesterol clefts were found in the periventricular regions of the lateral ventricle. However, the

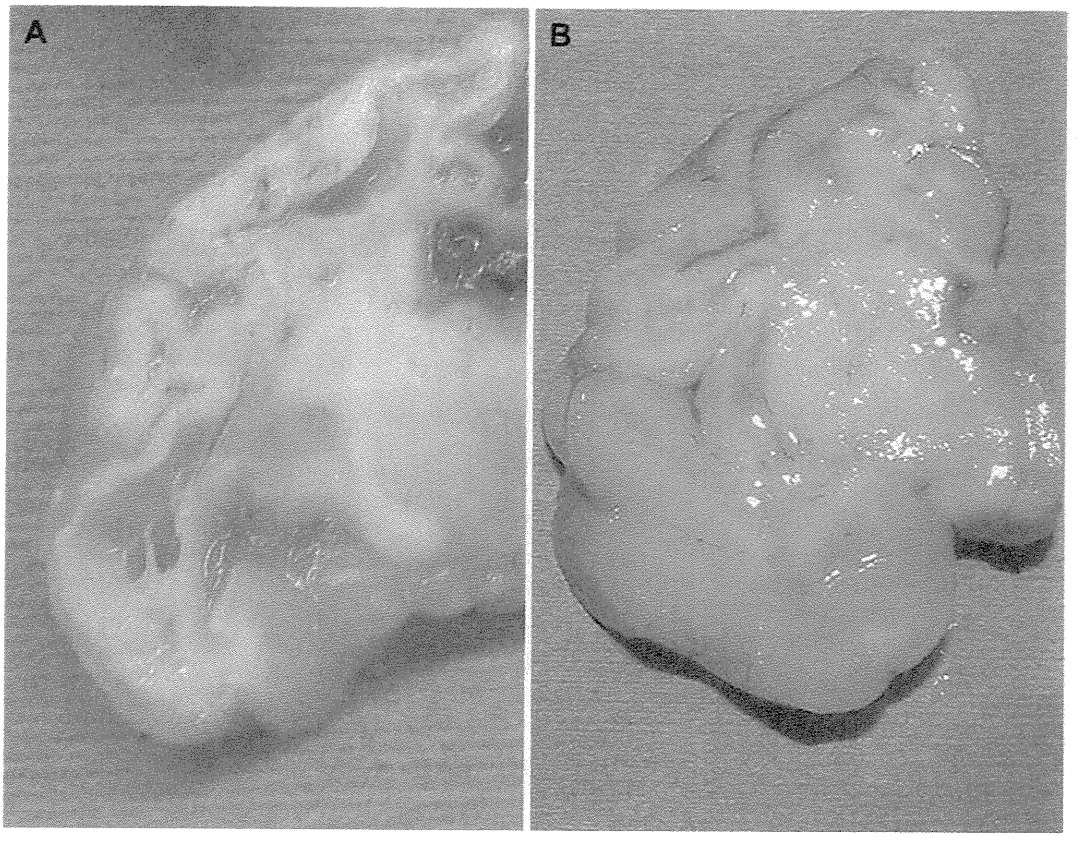

Fig. 1. (A) Cerebrum of a 21-day-old cynomolgus monkey (case 1). Marked cavitation of the white matter and atrophy of the cortical region are present in the temporal lobe. (B) Cerebrum in a 7-day-old cynomolgus monkey (case 2). Multiple foci of white matter softening are present in the temporal lobe.

periventricular regions and ependymal layers of the third ventricle appeared to be largely normal, except for a slight infiltration of glial cells. In case 2, the cerebrum showed massive liquefactive necrosis, with infiltration of lipid-filled phagocytes bilaterally in the temporal white matter and particularly in the periventricular areas of the lateral ventricle. Furthermore, there was diffuse reactive astrocytosis with gemistocytes (Fig. 3A) in various white matter areas and focally in the temporal deep gray matter. The density of neuronal cells was significantly reduced in the lesional sites. Periventricular areas of the third ventricle and thalamus also showed a decrease in neurons infiltration of lipid-filled phagocytes and astrocytosis. Examination of the brainstem, cerebellum, spinal cord and optic nerves did not reveal any abnormalities in either case.

In case 1, immunohistochemical labelling for expression of GFAP revealed apparent proliferation of glial fibrils in the cerebral cortex around cavitations or foci of liquefactive necrosis consistent with glial scar formation (Fig. 2B). In case 2, gemistocytes in the cerebral white matter displayed strong cytoplasmic immunoreactivity for GFAP (Fig. 3A). Immature astrocytes with narrow cytoplasm and long processes were immunolabelled for GFAP and vimentin (Fig. 3B) in the cerebral cortex and the cerebral white matter. Lipid-filled phagocytes in necrotic foci displayed granular cytoplasmic immunoreactivity for CD68 in both cases (Fig. 2A). Neurons displaying immunoreactivity for NF were significantly reduced in number in each case. Both cases were negative for Cas3 expression, suggesting that the lesions were a result of necrosis rather than apoptosis. Double immunohistochemical labelling with anti-MBP and anti-olig2 was also performed. In normal neonatal monkey brains, some oligodendroglial cells and many myelin sheaths were observed in the white matter (Fig. 4). In contrast, the white matter in case 2 showed a marked decrease in oligodendroglial cells and myelin sheaths (Fig. 4). The white matter in case 1 was unlabelled due to loss of all cellular elements within the areas of cavitation.

In case 1, the lung showed alveolar collapse with proliferation of type II alveolar epithelial cells (AEC II) and infiltration of macrophages into the alveolar space. In case 2, the lung showed severe diffuse pneumonia with infiltration of neutrophils and macrophages into the alveolar space and exfoliation of the alveolar epithelium.

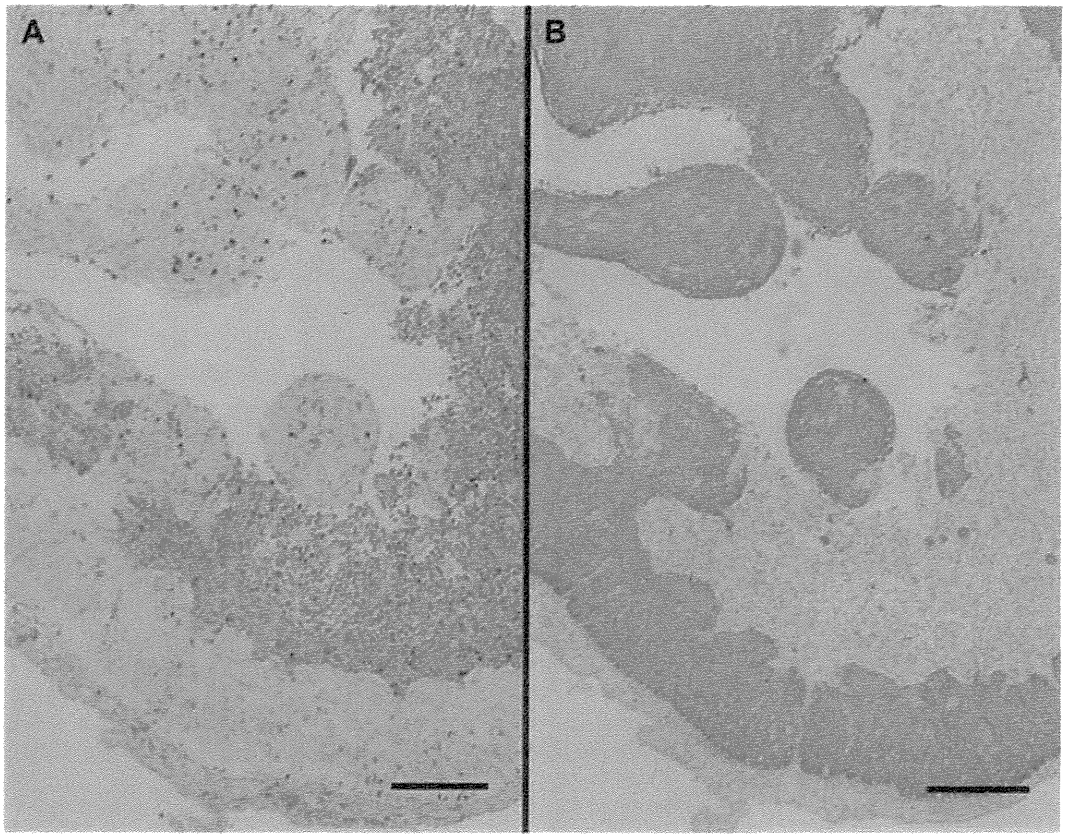

Fig. 2. Cerebrum of a 21-day-old cynomolgus monkey (case 1). (A) There is cavitation or foci of liquefactive necrosis with loss of all cellular elements from white matter to deep gray matter, with aggregation of many lipid-filled phagocytes expressing CD68 in the necrotic foci. IHC. Bar, 200 μm. (B) There is apparent proliferation of glial fibrils around these areas of cavitation or liquefactive necrosis. IHC. Bar, 200 μm.

Some colonies of gram-positive bacteria with morphology consistent with *Staphylococcus* were also observed within the white nodules in the lungs. Additionally, gastric contents, including milk, were found in the trachea of both cases. Atrophy of femoral muscles was observed with proliferation of stromal connective tissue in each case, and this change was particularly severe in case 1. The sciatic nerves of both monkeys appeared almost normal, but there was proliferation of surrounding perineural connective tissue.

Brain injury in the premature human infant consists of multiple lesions, principally germinal intraventricular haemorrhage, post-haemorrhagic hydrocephalus and PVL (Volpe, 2003). PVL refers to injury of the cerebral white matter that occurs with characteristic distribution and consists of focal periventricular necrosis with subsequent cyst formation (cystic PVL) and more diffuse cerebral white matter necrosis with subsequent glial scaring (non-cystic PVL). A third form of cerebral white matter abnormality (the third form of PVL) consists of diffuse astrogliosis without necrosis (Khwaja and Volpe, 2008). PVL is the major form of brain white matter injury that affects premature human infants and is associated with subsequent development of cerebral palsy, intellectual impairment and visual disturbances. There is currently no specific therapy for PVL (Pierson *et al.*, 2007). The diagnostic hallmarks of PVL are periventricular echodensities or cysts detected by cranial ultrasonography (Deng *et al.*, 2008). Two major factors appear to be involved in the development of PVL. The first involves fetal or neonatal hypoxia–ischaemia that can be a consequence of reduced blood flow to the umbilicus, uterus or placenta in the prenatal or perinatal period. Recent studies suggest that a disturbance of circulation, such as severe hypotension, or cardiogenic shock in preterm infants, such as caused by severe perinatal asphyxia, plays a decisive role in the formation of PVL-lesions (Shankaran *et al.*, 2006; Khwaja and Volpe, 2008). Moreover, experimental studies in which hypoxia is induced artificially have been also conducted in animals for exploration of the pathophysiology of PVL (Painter, 1995; Kohlhauser *et al.*, 2000). Anatomically, early in development, the deep penetrating arteries of the middle cerebral artery that supply the periventricular white matter lack the

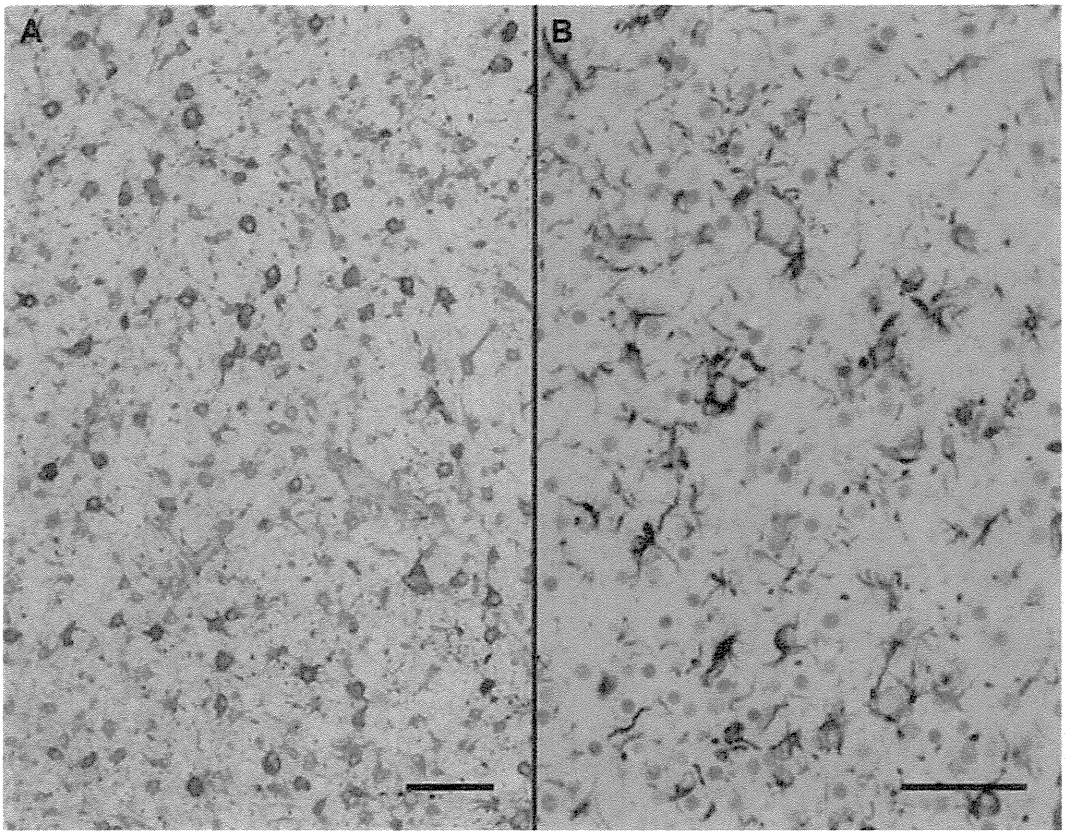

Fig. 3. Cerebrum of a 7-day-old cynomolgus monkey (case 2). (A) Large numbers of reactive astrocytes are present in the cerebral white matter. The cytoplasm of these cells labels for expression of GFAP, an astrocyte-specific marker. IHC. Bar, 50 μm. (B) Premature astrocytes are also present in the cerebral cortex. The narrow cytoplasm and long processes of these cells were immunolabelled for expression of vimentin. IHC. Bar, 50 μm.

vascular anastomoses that help maintain perfusion during periods of hypotension (Takashima *et al.*, 1978; Rorke, 1992; Inage *et al.*, 2000). Therefore, as cerebral autoregulation begins to fail following severe hypotension in neonatal infants, particularly in preterm infants, blood flow is selectively impaired and initially in the white matter of the periventricular region. Furthermore, there is recent evidence that the brain of sick preterm infants often shows impaired cerebrovascular autoregulation in response to change in blood pressure (Soul *et al.*, 2007). This selective hypoperfusion of cerebral white matter during severe hypotension provides a mechanistic explanation for the pathogenesis of PVL. Meanwhile, microglia are activated by the release of reactive oxygen species (ROS) and reactive nitrogen species (RNS), which may mediate cell death. The reactive astrocytes in diffuse lesions could also contribute to the formation of RNS. The release of ROS and RNS by microglia seems likely to result in death of premyelinating oligodendrocytes (pre-OLs) or prevent pre-OLs from differentiating to mature myelin-producing cells in the injured cerebral white matter (Volpe, 2003; Khwaja and Volpe, 2008).

The second major factor contributing to the development of PVL is thought to be maternal intrauterine (or neonatal) infection and fetal (or neonatal) systemic inflammation. Increasing numbers of studies have implicated intrauterine infection in the genesis of PVL. Recent investigations have shown that intravenous injection of the bacterial endotoxin lipopolysaccharide (LPS) can produce selective white matter injury in the neonatal CNS (Paintlia *et al.*, 2008), whereas induction of intrauterine infection can produce diffuse glial cell death and cavitation in fetal white matter (Sherwin and Fern, 2005). The secretion of proinflammatory cytokines such as interleukin (IL)-1, IL-6, and tumor necrosis factor (TNF)-α is known to be toxic to the developing fetal brain (Damman and Levinton, 1997) and may lead to astrogliosis affecting the maturation of myelin-forming oligodendrocytes (Leviton and Gilles, 1996).

The gestation period of the cynomolgus monkey averages 165 days in the TPRC. Case 1 was born on day 163 of gestation and was thus of normal gestational age; however, this animal suffered from a period of asphyxia due to perinatal dystocia. Perinatal asphyxia results from oxygen deprivation that may

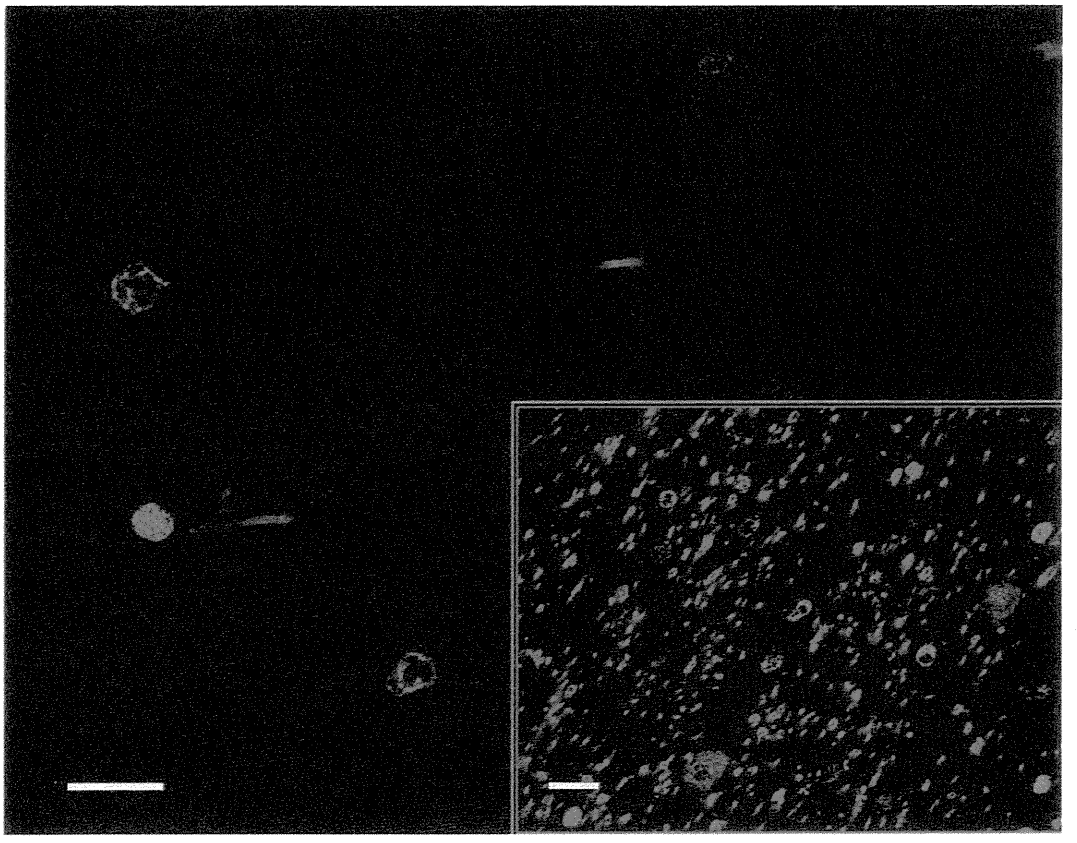

Fig. 4. Cerebrum of a 7-day-old cynomolgus monkey (case 2). Sections were double labelled with antibodies specific for MBP (green) and olig2 (red). There is reduction in cells expressing olig2 and almost no expression of MBP in the cerebral white matter. IHC. Bar, 10 μm. Inset: cerebrum of a normal 0-day-old cynomolgus monkey double labelled as above (control). Within the white matter, oligodendroglial cells express olig2 and many myelin sheaths express MBP. IHC. Bar, 10 μm.

cause harm to the neonatal infant. The condition occurs most commonly due to a drop in maternal blood pressure or interference with blood flow to the brain of the infant during delivery. This was likely to have been the aetiology of the lesions observed in the brain of case 1.

Case 2 was born 16 days before the expected date of confinement. Although PVL may occur in term infants, the injury is more common in premature infants, especially those born between 26 and 34 weeks of gestation (Locatelli *et al.*, 2005). The brain injury in preterm infants is mainly due to the oxidative stress placed on the neonate during delivery (Robles *et al.*, 2001; Haynes *et al.*, 2005), the immaturity of the developing nervous system, and the immaturity of the cerebrovascular supply (Khwaja and Volpe, 2008). Robles *et al.* (2001) investigated the concentration of hydroperoxides, which are measures of oxidative stress. These authors demonstrated that full-term neonates had levels of hydroperoxides that dropped sharply in the first few hours following birth. However, in premature infants the concentration of hydroperoxides remained at near birth levels for as long as a week and at dangerously high levels for even longer. Therefore, preterm neonates are at risk of free-radical injury during this period. In addition to these underlying factors, hypoxia–ischaemia can lead to more free-radical production, which can then damage the pre-OLs (Yoshida-Shuto *et al.*, 1992; Robles *et al.*, 2001). Thus, case 2 was at risk of a nervous system disorder and was of especially high risk for developing PVL. A genetic susceptibility to PVL has been proposed with cytokine genes acting as risk modifiers (Baier, 2006), but there was no familial association between the two animals of the present report.

Case 1 had marked cavitation with loss of cellular elements in the cerebral white matter. These changes are similar to cystic PVL and the cavitations may be formed by fusion of multiple cystic foci. Case 2 did not show cavitation, despite the presence of diffuse necrosis of the cerebral white matter, astrogliosis, decreased oligodendroglial cells and marked dysmyelination. These changes are similar to non-cystic PVL or the third form of PVL, and dysmyelination must have been caused by a decrease of myelin-producing oligodendrocytes and disturbance of pre-OL maturation.

The pathological differences between the two monkeys may also have been influenced by the duration of ischaemia or other factors such as fetal age or the length of survival. In general, it is said that microglial reactivity is apparent within 24 h, peaks at 7 days and remains present for weeks following the ischaemia. Phenotypic changes in resident astrocytes occur at 24 h, and these cells proliferate between 48 h and 7 days after ischaemia. Over the ensuing weeks and months, astrocytes increase in number and in fibrillary appearance, eventually resulting in a glial scar or cavitation (Cervós-Navarro and Lafuente, 1991; Williams *et al.*, 2007). Case 1 had widespread cavitation and severe glial scarring, while case 2 showed neuronal decrease, infiltration of lipid-filled phagocytes and astrocytosis in the cerebral white matter and the thalamus. The thalamus is commonly affected in premature infants with PVL (Volpe, 2009), therefore the thalamic lesion in case 2 may have been linked to preterm birth. Furthermore, in each case the femoral muscles showed apparent neurogenic atrophy, likely secondary to dysfunction of the cerebral white matter.

Both monkeys had diffuse pulmonary lesions. In case 1, alveolar collapse was observed with proliferation of AEC II. This may have been caused by artificial ventilation and inhalation of highly concentrated oxygen administered as part of the medical care of the animal. Hyperoxia or hypocarbia results in the death of AEC I and subsequent proliferation of AEC II that differentiate to AEC I to replace the injured or dead AECs during the recovery stages (Takemura and Akamatsu, 1987). Case 2 showed severe purulent alveolar pneumonia with bacterial infection. This bacterial pneumonia may have been due to compromise of the immune system or decreased strength in this premature infant. Both tracheas were filled with a mixture of milk and mucus, suggesting that the animals may have terminally aspirated gastric contents.

Criteria for PVL in animals have not been defined, but the clinical and pathological features of our cases were very similar to those of PVL in man. TPRC has a large-scale breeding colony of experimental cynomolgus monkeys, with about 200 births each year. However, these are the first cases experienced in the TPRC and the first from any primate centre. Future cases should also be subject to ultrasonographic or magnetic resonance imaging investigation. Brain injury in premature infants has an enormous importance to public health because of the large number of such infants who survive with serious neurodevelopmental disability, including major cognitive deficits and motor disability. Because man and monkeys are very similar in anatomy, motor function and cognitive ability, monkeys are favoured as non-human primate models for the study of post-injury changes in the CNS. These spontaneously arising cases in non-human primates will contribute greatly to understanding the pathophysiology of PVL and to the development of an effective therapy for PVL or cerebral palsy.

Acknowledgments

This study was supported by the Tsukuba Primate Research Center, National Institute of Biomedical Innovation, Japan.

References

Baier RJ (2006) Genetics of perinatal brain injury in the preterm infant. *Frontiers in Biosciences*, **11**, 1371–1387.

Brazel CY, Rosti RT, Boyce S, Rothstein RP, Levison SW (2004) Perinatal hypoxia/ischemia damages and depletes progenitors from the mouse subventricular zone. *Developmental Neuroscience*, **26**, 266–274.

Cervós-Navarro J, Lafuente JV (1991) Traumatic brain injuries: structural changes. *Journal of Neurological Science*, **103**, S3–S14.

Damman O, Levinton A (1997) Maternal intrauterine infection, cytokines, and brain damage in the preterm newborn. *Pediatric Research*, **42**, 1–8.

Deng W, Pleasure J, Pleasure D (2008) Progress in periventricular leukomalacia. *Archives of Neurology*, **65**, 1291–1295.

Haynes RL, Baud O, Li J, Kinney HC, Volpe JJ *et al.* (2005) Oxidative and nitrative injury in periventricular leukomalacia: a review. *Brain Pathology*, **15**, 225–233.

Inage YW, Itoh M, Takashima S (2000) Correlation between cerebrovascular maturity and periventricular leukomalacia. *Pediatric Neurology*, **22**, 204–208.

Khwaja O, Volpe JJ (2008) Pathogenesis of cerebral white matter injury of prematurity. *Archives of Disease in Childhood. Fetal and Neonatal Edition*, **93**, 153–161.

Kohlhauser C, Mosgöller W, Höger H, Lubec B (2000) Myelination deficits in brain of rats following perinatal asphyxia. *Life Sciences*, **67**, 2355–2368.

Levison SW, Rothstein RP, Romanko MJ, Snyder MJ, Meyers RL *et al.* (2001) Hypoxia/ischemia depletes the rat perinatal subventricular zone of oligodendrocyte progenitors and neural stem cells. *Developmental Neuroscience*, **23**, 234–247.

Leviton A, Gilles F (1996) Ventriculomegaly, delayed myelination, white matter hypoplasia, and 'periventricular' leukomalacia: how are they related? *Pediatric Neurology*, **15**, 127–136.

Locatelli A, Ghidini A, Paterlini G, Patanè L, Doria V *et al.* (2005) Gestational age at preterm premature rupture of membranes: a risk factor for neonatal white matter damage. *American Journal of Obstetrics and Gynecology*, **193**, 947–951.

Painter MJ (1995) Animal models of perinatal asphyxia: contributions, contradictions, clinical relevance. *Seminars in Pediatric Neurology*, **2**, 37–56.

Paintlia MK, Paintlia AS, Contreras MA, Singh I, Singh AK (2008) Lipopolysaccharide-induced

peroxisomal dysfunction exacerbates cerebral white matter injury: attenuation by N-acetyl cysteine. *Experimental Neurology*, **210**, 560–576.

Pierson CR, Folkerth RD, Billiards SS, Trachtenberg FL, Drinkwater ME *et al.* (2007) Gray matter injury associated with periventricular leukomalacia in the premature infant. *Acta Neuropathology*, **114**, 619–631.

Rentmeister K, Schmidbauer S, Hewicker-Trautwein M, Tipold A (2004) Periventricular and subcortical leukoencephalopathy in two dachshund puppies. *Journal of Veterinary Medicine Series A: Physiology, Pathology and Clinical Medicine*, **51**, 327–331.

Resch B, Jammernegg A, Vollaard E, Maurer U, Mueller WD *et al.* (2004) Preterm twin gestation and cystic periventricular leucomalacia. *Archives of Disease in Childhood. Fetal and Neonatal Edition*, **89**, F315–320.

Robles R, Palomino N, Robles A (2001) Oxidative stress in the neonate. *Early Human Development*, **65**, S75–S81.

Rorke LB (1992) Anatomical features of the developing brain implicated in pathogenesis of hypoxic-ischemic injury. *Brain Pathology*, **2**, 211–221.

Shankaran S, Langer JC, Kazzi SN, Laptook AR, Walsh M (2006) Cumulative index of exposure to hypocarbia and hyperoxia as risk factors for periventricular leukomalacia in low birth weight infants. *Pediatrics*, **118**, 1654–1659.

Sherwin C, Fern R (2005) Acute lipopolysaccharide-mediated injury in neonatal white matter glia: role of TNF-alpha, IL-1beta, and calcium. *Journal of Immunology*, **175**, 155–161.

Soul JS, Hammer PE, Tsuji M, Saul JP, Bassan H *et al.* (2007) Fluctuating pressure-passivity is common in the cerebral circulation of sick premature infants. *Pediatric Research*, **61**, 467–473.

Takashima S, Armstrong DL, Becker LE (1978) Subcortical leukomalacia. Relationship to development of the cerebral sulcus and its vascular supply. *Archives of Neurology*, **35**, 470–472.

Takemura T, Akamatsu H (1987) Ultrastructural study on the pulmonary parenchyma of the neonates following prolonged mechanical ventilation. *Acta Pathologica Japonica*, **37**, 1115–1126.

Volpe JJ (2003) Cerebral white matter injury of the premature infant – more common than you think. *Pediatrics*, **112**, 176–180.

Volpe JJ (2009) Brain injury in premature infants: a complex amalgam of destructive and developmental disturbances. *Lancet Neurology*, **8**, 110–124.

Williams AJ, Wei HH, Dave JR, Tortella FC (2007) Acute and delayed neuroinflammatory response following experimental penetrating ballistic brain injury in the rat. *Journal of Neuroinflammation*, **2**, 4–17.

Yoshida-Shuto H, Yasuhara A, Kobayashi Y (1992) Cerebral blood flow velocity and failure of autoregulation in neonates: their relation to outcome of birth asphyxia. *Neuropediatrics*, **23**, 241–244.

Young RS, Hernandez MJ, Yagel SK (1982) Selective reduction of blood flow to white matter during hypotension in newborn dogs: a possible mechanism of periventricular leukomalacia. *Annals of Neurology*, **12**, 445–448.

[*Received, January 23rd, 2010*
Accepted, June 27th, 2010]

ELSEVIER

INSTITUT PASTEUR

Microbes and Infection 13 (2011) 58–64

www.elsevier.com/locate/micinf

Original article

Improved capacity of a monkey-tropic HIV-1 derivative to replicate in cynomolgus monkeys with minimal modifications

Akatsuki Saito [a,b,c,1], Masako Nomaguchi [d,1], Sayuki Iijima [c], Ayumu Kuroishi [e], Tomoyuki Yoshida [b], Young-Jung Lee [c], Toshiyuki Hayakawa [b], Ken Kono [e], Emi E. Nakayama [e], Tatsuo Shioda [e], Yasuhiro Yasutomi [c], Akio Adachi [d], Tetsuro Matano [a], Hirofumi Akari [b,c,*]

[a] *International Research Center for Infectious Diseases, The Institute of Medical Science, The University of Tokyo, Tokyo 108-8639, Japan*
[b] *Primate Research Institute, Kyoto University, Inuyama 484-8506, Japan*
[c] *Tsukuba Primate Research Center, National Institute of Biomedical Innovation, Tsukuba 305-0843, Japan*
[d] *Department of Microbiology, Institute of Health Biosciences, The University of Tokushima Graduate School, Tokushima 770-8503, Japan*
[e] *Department of Viral Infections, Research Institute for Microbial Diseases, Osaka University, Suita 565-0871, Japan*

Received 31 July 2010; accepted 1 October 2010
Available online 16 October 2010

Abstract

Human immunodeficiency virus type 1 (HIV-1) hardly replicates in Old World monkeys. Recently, a mutant HIV-1 clone, NL-DT5R, in which a small part of *gag* and the entire *vif* gene are replaced with SIVmac239-derived ones, was shown to be able to replicate in pigtail monkeys but not in rhesus monkeys (RM). In the present study, we found that a modified monkey-tropic HIV-1 (HIV-1mt), MN4-5S, acquired the ability to replicate efficiently in cynomolgus monkeys as compared with the NL-DT5R, while neither NL-DT5R nor MN4-5S replicated in RM cells. These results suggest that multiple determinants may be involved in the restriction of HIV-1 replication in macaques, depending on the species of macaques. The new HIV-1mt clone will be useful for studying molecular mechanisms by which anti-viral host factors regulate HIV-1 replication in macaques.

Keywords: HIV-1; Old World monkey; TRIM5α

1. Introduction

Human immunodeficiency virus type 1 (HIV-1) productively infects only humans but not Old World monkeys (OWM) such as cynomolgus monkeys (CM) or rhesus monkeys (RM), whereas RM-derived simian immunodeficiency virus (SIVmac) can efficiently replicate in OWM. Because of this species barrier, alternative monkey models using SIVmac or simian/human immunodeficiency viruses (SHIV) have been used for AIDS research [1–4]. However, detailed analyses of molecular mechanisms of the pathogenesis of HIV-1 have been hampered by the lack of appropriate non-human primate models for HIV-1 infection.

The mechanistic basis for the inability of HIV-1 to replicate in OWM cells has remained unclear. Recently, a number of intrinsic anti-HIV-1 cellular factors, including tripartite motif protein 5α (TRIM5α), Cyclophilin A (CypA), apolipoprotein B mRNA-editing catalytic polypeptide (APOBEC3) family and Tetherin were discovered in OWM cells [5,6]. TRIM5α strongly suppresses HIV-1 replication, mainly by affecting the viral disassembly step, resulting in a decrease of reverse transcription products [7,8]. CypA acts as a regulator promoting TRIM5α-mediated restriction of HIV-1 [8]. APOBEC3 is also a major regulator of HIV-1 replication [9,10]. APOBEC3 exerts its inhibitory effect mainly by inducing G to A hypermutation

* Corresponding author. Primate Research Institute, Kyoto University, Inuyama 484-8506, Japan. Tel.: +81 568 63 0440; fax: +81 568 63 0459.
E-mail address: akari@pri.kyoto-u.ac.jp (H. Akari).
[1] A.S. and M.N. contributed equally to this work.

1286-4579/$ - see front matter © 2010 Institut Pasteur. Published by Elsevier Masson SAS. All rights reserved.
doi:10.1016/j.micinf.2010.10.001

into the viral genome due to its cytidine deaminase activity, while hypermutation-independent inhibitory activity at the stage of reverse transcription is also evident [11]. Tetherin, also referred to as a BST-2, was identified as an intrinsic anti-viral factor that restricts the egress of HIV-1 by tethering virions to the host cell surface [12,13]. Importantly, HIV-1 can counteract human APOBEC3 activity by utilizing the viral accessory protein Vif, whereas it cannot counteract OWM APOBEC3 [14]. Similarly, HIV-1 counteracts human Tetherin activity by utilizing another viral accessory protein Vpu, whereas HIV-1 does not counteract OWM Tetherin activity [15].

In an attempt to generate a monkey-tropic HIV-1 (HIV-1mt), Kamada et al. constructed an HIV-1 variant carrying minimal SIVmac-derived sequences to overcome the restriction factors [16]. The prototype HIV-1 clone NL-DT5R had a sequence encoding an SIVmac loop between alpha helices 4 and 5 (L4/5) of *capsid* gene (CA) and the entire *vif* gene, which relieved the inhibitory effects on viral replication by restriction factors CypA, TRIM5α and APOBEC3. NL-DT5R was able to replicate in pigtail monkeys (PM) in vivo as well as in vitro, as reported by Igarashi et al. [17]. Although NL-DT5R induced immune responses in infected animals, the virus did not establish persistent infection.

In the present study, we sought to adapt NL-DT5R to CM by performing long-term passage in CM-derived HSC-F cells. We successfully obtained a modified HIV-1mt clone having several mutations. Additionally, we inserted an SIVmac loop between alpha helices 6 and 7 (L6/7) of CA [18]. The resultant clone named MN4-5S was found to replicate efficiently and to induce strong immune responses in infected CM, suggesting the impact of viral adaptation.

2. Materials and methods

2.1. Plasmid construction

The HIV-1 derivatives were constructed on a background of an infectious molecular clone, NL4-3 [19]. NL-DT5R, a cloned virus containing SIVmac239 L4/5 and the entire *vif* gene, was reported previously by Kamada et al. [16]. In addition, NL-DT562, a virus having an R5-tropic SF162-derived *env* gene on a background of NL-DT5R, was used in this study [20]. After long passage of NL-DT5R and NL-DT562 in cynomolgus T cell line HSC-F [21], several mutations were appeared in both viral genomes, and then all of them were inserted into NL-DT5R by gene-engineering techniques. Consequently, a clone having 14 nucleotide substitutions in its genome was constructed and named MN4-5. Among these substitutions, 7 were non-synonymous mutations. The structure of the clone is shown in Fig. 1. A part of L6/7 of CA (aa residues 120–122; HNP) of MN4-5 was also replaced with the corresponding segment of SIVmac239 CA (aa residues 120–123; RQQN) by means of site-directed mutagenesis as described previously in Ref. [18]. The resultant construct was designated MN4-5S.

2.2. Cells and viruses

Human embryonic kidney cell line HEK293T was maintained in DMEM supplemented with 10% fetal bovine serum, 100 units/ml of penicillin and 100 μg/ml of streptomycin (Sigma). Monkey peripheral blood mononuclear cells (PBMCs) were separated with a standard Ficoll density gradient separation method and cultured in R-10 composed of

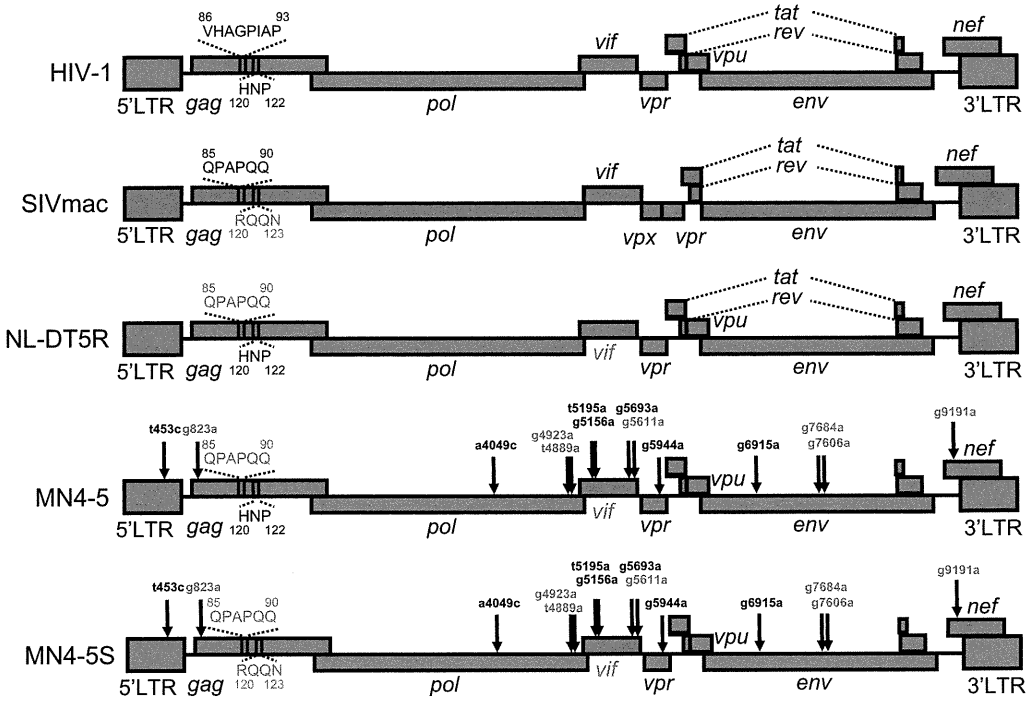

Fig. 1. Structure of HIV-1mt clones used in this study. The positions of nucleotide mutations are indicated by arrows in this figure. Among nucleotide substitutions, the positions of non-synonymous mutations are indicated in red.

RPMI-1640 medium supplemented with 10% fetal bovine serum, 100 units/ml of penicillin and 100 μg/ml of streptomycin (Sigma). The growth kinetics of each HIV-1 clone were examined in activated $CD8^+$ cell-depleted PBMCs. Briefly, separated PBMCs were reacted with a PE-labeled anti-CD8 antibody and then treated with anti-PE magnetic beads. After washing, $CD8^+$ cell-depleted PBMCs were negatively separated by using MACS columns (Miltenyi Biotec). For stimulation, $CD8^+$ cell-depleted PBMCs were first cultured in R-10 containing 1 μg/ml of concanavalin A (Sigma) for 2 days followed by culture in R-10 supplemented with 100 U/ml IL-2 (Shionogi) for more 2 days. The cells were then infected with 100 ng of p24 of HIV-1 and the culture supernatant was collected periodically. HSC-F, a cynomolgus monkey-derived $CD4^+$ T cell line [21], was cultured in R-10.

Virus stocks were prepared as follows: sub-confluent HEK293T cells were transfected with proviral DNA using Lipofectamine2000 reagent according to the manufacturer's instructions. At 42 h after transfection, culture supernatants were centrifuged, filtrated with a 0.45 μm filter, and aliquoted as virus stocks for in vitro experiments. For preparation of viral stocks for in vivo experiments, $CD8^+$ cell-depleted PBMCs were infected with the HEK293T-derived stocks as described above. After washing, the cells were maintained for several days and the culture supernatants were collected and stored as described above.

2.3. Reverse transcription (RT) assay

Virion-associated RT activity was measured as described previously in Ref. [22]. HSC-F cells (1×10^6) were infected with equal amounts of viruses (1×10^7 RT units). Viral growth kinetics was determined by RT production in the culture supernatants.

2.4. Animal experiments

Healthy adult cynomolgus monkeys were used in this study. All animals were confirmed to be negative for simian retrovirus and were housed in individual isolators in a biosafety level 3 facility and maintained according to the National Institute of Biomedical Innovation rules and guidelines for experimental animal welfare. Bleeding and viral inoculation were performed under ketamine hydrochloride anesthesia. Viral stocks for inoculation were inoculated into each animal. The profiles of plasma viral RNA loads, circulating $CD4^+$ and $CD8^+$ T lymphocytes were evaluated as described below.

2.5. Flow cytometry and immunophenotyping of peripheral blood lymphocytes

Immunophenotyping of freshly isolated PBMCs was performed according to standard procedures using multicolor flow cytometry performed with a FACSCantoII (Becton Dickinson). $CD4^+$ and $CD8^+$ T cells were identified using monoclonal antibodies (mAbs) to CD3 (clone SP34-2, BD Pharmingen), CD4 (clone L200, BD Pharmingen) and CD8 (clone DK25, DAKO). Flow cytometric acquisition and analysis of samples was performed on at least 10,000 events collected by a flow cytometer driven by FACSDiVa software.

2.6. Analysis of anti-viral antibody response

Plasma samples from infected animals were first heat-inactivated at 56 °C for 30 min. Then, 100-fold diluted samples were reacted with commercially available anti-HIV-1 antibody detection strips (New LAV Blot I, Bio-Rad) according to the manufacture's instructions.

2.7. In vivo depletion of $CD8^+$ lymphocytes

Infected animals received an anti-CD8 mAb (cM-T807) as follows: 10 mg/kg (body weight) inoculation subcutaneously at 42 days post infection (DPI), followed by 5 mg/kg inoculation intravenously at 45, 49, and 52 DPI. The cM-T807 mAb was provided by the NIH Nonhuman Primate Reagent Resource. To repeatedly confirm the depletion of $CD8^+$ cells in the presence of cM-T807, an anti-CD8 mAb (clone DK25, DAKO) was used as reported previously in Ref. [23].

2.8. Quantification of viral RNA

Total RNA was collected from monkey plasma using a High Pure Viral RNA Kit (Roche Diagnostics) according to the manufacturer's instructions. Viral RNA was quantified with a quantitative real-time PCR system using TaqMan One-Step RT-PCR Master Mix Reagents (Applied Biosystems). The primers and probe used in this study were as follows: Forward primer: HIVgag683 (+) (5′-CTCTCGACGCAGGACTCGGCTTGCT-3′); Reverse primer: HIVgag803 (−) (5′-GCTCTCGCACCCATCTCTCTCCTTCTAGCC-3′); Probe: HIVgag TaqMan 720R748 (FAM-GCAAGAGGCGAGRGGCGGCGACTGGTGAG-TAMRA). The quantification and data analysis were performed using the iQ5 Real-Time PCR Detection System (Bio-Rad). The detection limit of this assay was 400-copies/ml plasma.

3. Results

3.1. Growth properties of prototype HIV-1mt clone, NL-DT5R in macaques in vitro and in vivo

We first examined the replication properties of prototype HIV-1mt NL-DT5R in $CD8^+$ cell-depleted PBMCs of CM and RM. NL-DT5R replicated in the cells of CM but not in those of RM (Fig. 2). We next examined the in vivo replication properties of NL-DT5R in CM. Viral stocks for inoculation were prepared with $CD8^+$ cell-depleted CM PBMCs as described above. Then, two monkeys were infected with NL-DT5R intravenously and bled periodically. As shown in Fig. 3A, NL-DT5R established infection as indicated by detectable levels of plasma viremia and an anti-HIV-1 antibody response, although the viral level was marginal (about 1×10^3 copies/ml) and disappeared at 4 weeks post infection.

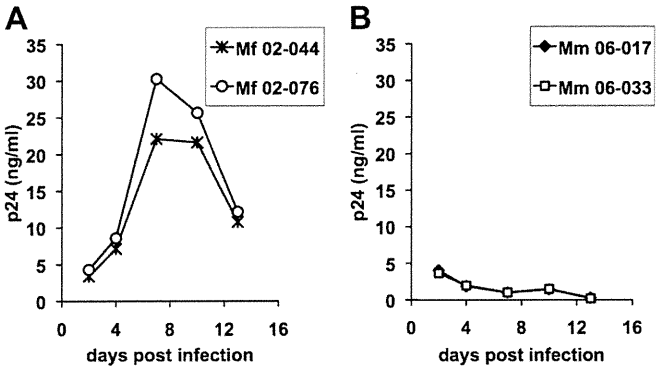

Fig. 2. Growth properties of the NL-DT5R in CD8$^+$ cell-depleted PBMCs from CM (A) and RM (B). The cells were infected with NL-DT5R and the viral replication was monitored by p24 antigen in the culture supernatants using a p24 quantitative ELISA kit. Animal identifications are indicated at the top of each panel.

These results indicated that although CM appeared permissive for NL-DT5R as compared with RM, the mutations introduced in NL-DT5R were not still sufficient to overcome the restriction by host factor(s) of these macaques.

3.2. MN4-5S showed improved replication capability in CM CD8$^+$ cell-depleted PBMCs

In order to improve the replication capability of HIV-1mt in CM, we conducted long-term passage of NL-DT5R in HSC-F cells. Additionally, NL-DT562, having an R5-tropic *env* gene on a background of NL-DT5R, was also passaged long-term in HSC-F cells. We found that the passaging improved the growth of the viruses (data not shown), and then viral clones were obtained after the long-term passaging and sequenced. Ten nucleotide substitutions were identified in the NL-DT5R-derived clone and 4 nucleotide substitutions (except for the *env* gene) in the NL-DT562-derived clone. These 14 nucleotide substitutions (7 of which were non-synonymous mutations) were assembled and introduced into NL-DT5R. The resultant clone was named MN4-5, and its structure is shown in Fig. 1. We previously found that insertion of an SIVmac loop between alpha helices 6 and 7 (L6/7) of CA into the corresponding region in HIV-1 significantly enhanced the viral replication in HSC-F cells and PBMCs of CM by relieving the inhibitory effect of TRIM5α [18]. We therefore inserted an SIVmac-derived L6/7 sequence into MN4-5. The resultant clone was named MN4-5S (Fig. 1). In order to examine the impact of these modifications on the viral replication, we analyzed the replication properties of this "adapted" virus in HSC-F cells and CD8$^+$ cell-depleted PBMCs of CM. MN4-5 showed higher replication as compared with NL-DT5R in both types of cells (Figs. 4 and 5). Moreover, MN4-5S showed enhanced growth capability in the cells as compared with the parental clones, NL-DT5R and MN4-5 (Figs. 4 and 5).

Notably, MN4-5S did not show any replication in RM cells (data not shown), indicating that the combination of the mutations introduced in NL-DT5R may be effective for escape from the restriction in CM cells but not in RM cells.

3.3. MN4-5S induced greater viremia in CM as compared with parental clone, NL-DT5R

Since MN4-5S showed enhanced ability to replicate in CM cells, we next examined the viral replication in vivo. The stock of MN4-5S virus was inoculated into 3 CM. MN4-5S induced 10-fold higher viremia in infected animals at 2–3 weeks after infection (Fig. 6A), as compared with that induced by NL-DT5R (see Fig. 3). This result was consistent with the in vitro result (Fig. 5) and demonstrated that the mutations inserted into NL-DT5R contributed to enhancement of viral replication in vivo. In addition, at the acute phase of infection a slight decrease of CD4$^+$ T cells was observed (Fig. 6B). The viremia became undetectable at 6 weeks after infection.

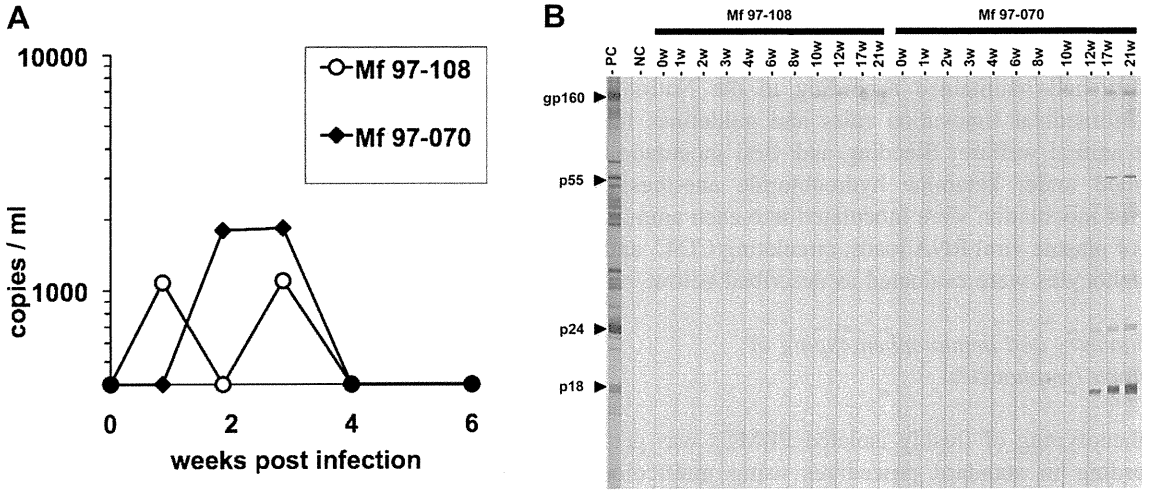

Fig. 3. Profiles of plasma viral RNA loads (A) and anti-HIV-1 antibody responses (B) in CM infected with NL-DT5R. Mf97-108 (open circles) and Mf97-070 (closed diamonds) were used in this study. Viral stocks for inoculation were prepared in CD8$^+$ cell-depleted PBMCs, and then 6.1 ng p24 of HIV-1 were inoculated into each animal. Commercially available diagnostic HIV-1 Western blotting strips were reacted with 100-fold diluted monkey plasma. Plasma from HIV-1-infected or uninfected individuals was used as a positive or a negative control, respectively.

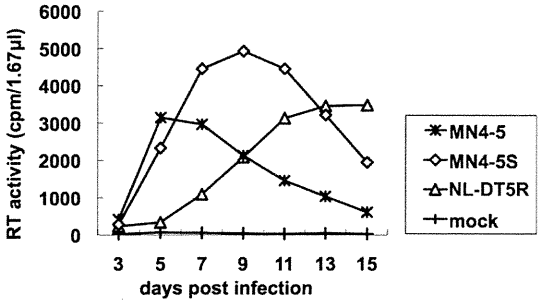

Fig. 4. Growth properties of HIV-1mt in HSC-F cells. The cells were infected with a series of HIV-1mt derivatives. The viral replication was monitored by RT activity in the culture supernatants.

Thereafter, antibody response against MN4-5S was observed in infected animals (Fig. 6C). As indicated by comparison with the lane of the positive control as a standard, the degree of antibody response seemed to be stronger than that against NL-DT5R (see Figs. 3B and 6C). Next we attempted to clarify the role of $CD8^+$ lymphocytes in the disappearance of viremia. We conducted in vivo depletion of $CD8^+$ cells by using a method reported previously [23]. We found that the reappearance of viremia was observed in all monkeys tested in parallel with the decline of $CD8^+$ T cells after the anti-CD8 mAb administration (Fig. 6A and D). This result indicated that $CD8^+$ T cells had a critical role in the control of HIV-1mt replication and suggested that the virus was able to infect latently in vivo.

4. Discussion

In the present study, we found that a modified HIV-1mt, MN4-5S, acquired greater ability to replicate in CM than NL-DT5R, and that both the SIVmac-derived L6/7 (HNP120-122 > RQQN120-123 of CA) and a series of substitutions identified by long-term passage of NL-DT5R in HSC-F cells contributed to this ability (Fig. 1). We recently showed that the substitution of L6/7 relieved the inhibitory effect of TRIM5α [18]. Additionally, our preliminary data suggest that non-synonymous mutations in the *integrase* and *env* genes are likely to be critical for the improved activity (Nomaguchi et al., manuscript in preparation). It is possible that these adaptive mutations may optimize the interaction between host and viral proteins.

It seemed that the growth kinetics of NL-DT5R in PM were comparable with those of MN4-5S in CM, which had peak levels in acute viremia of approximately 10^4 copies/ml [17]. It is therefore likely that PM may exhibit better susceptibility to HIV-1mt than CM. It is possible that the greater susceptibility of PM to HIV-1mt replication could be due to the genotype of TRIM5, because PM usually expresses a chimera between TRIM5α and CypA, so-called TRIM-Cyp, whose anti-HIV-1 activity is defective [24].

One unexpected finding in this study was that MN4-5S was unable to replicate in PBMCs of RM (data not shown), which was in contrast with the greater susceptibility of RM to SIV-mac infection. Our results suggested that RM was most resistant to HIV-1mt replication among the three macaque species. Since our HIV-1mt clones (NL-DT5R and MN4-5) were established on the basis of information obtained from serial passages of the viruses in CM-derived cells, it may be reasonable to consider that these viruses were consequently optimized to CM. Alternatively, it is also possible that anti-HIV-1 activities such as TRIM5α and APOBEC3 of RM could be greater than those of other macaques. Further studies are in progress to address these questions.

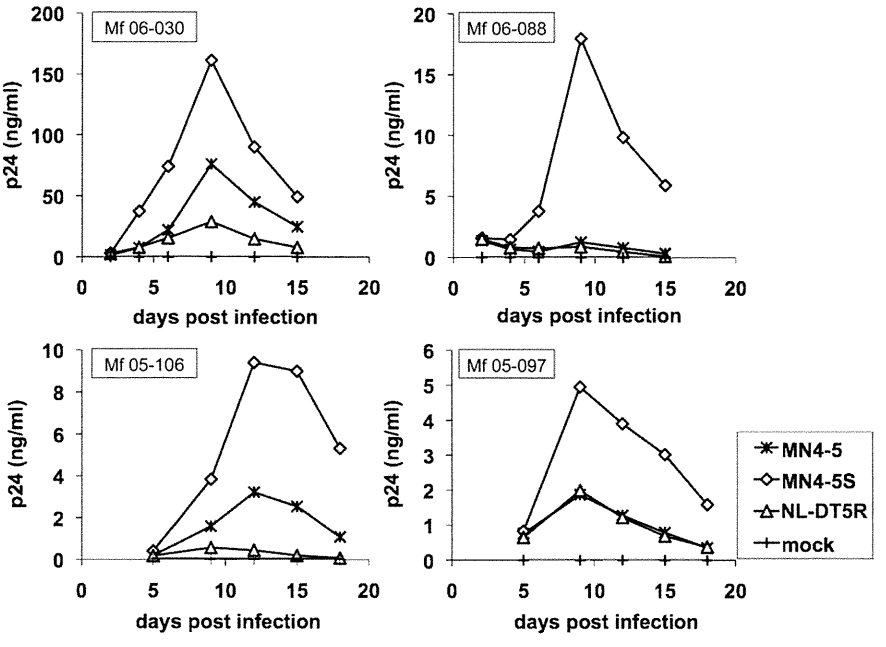

Fig. 5. Growth properties of HIV-1mt in $CD8^+$ cell-depleted PBMCs from four CM. The cells were infected with a series of HIV-1mt derivatives. The viral replication was monitored by p24 antigen in the culture supernatants using a p24 quantitative ELISA kit. Animal identifications are indicated at the top of each panel.

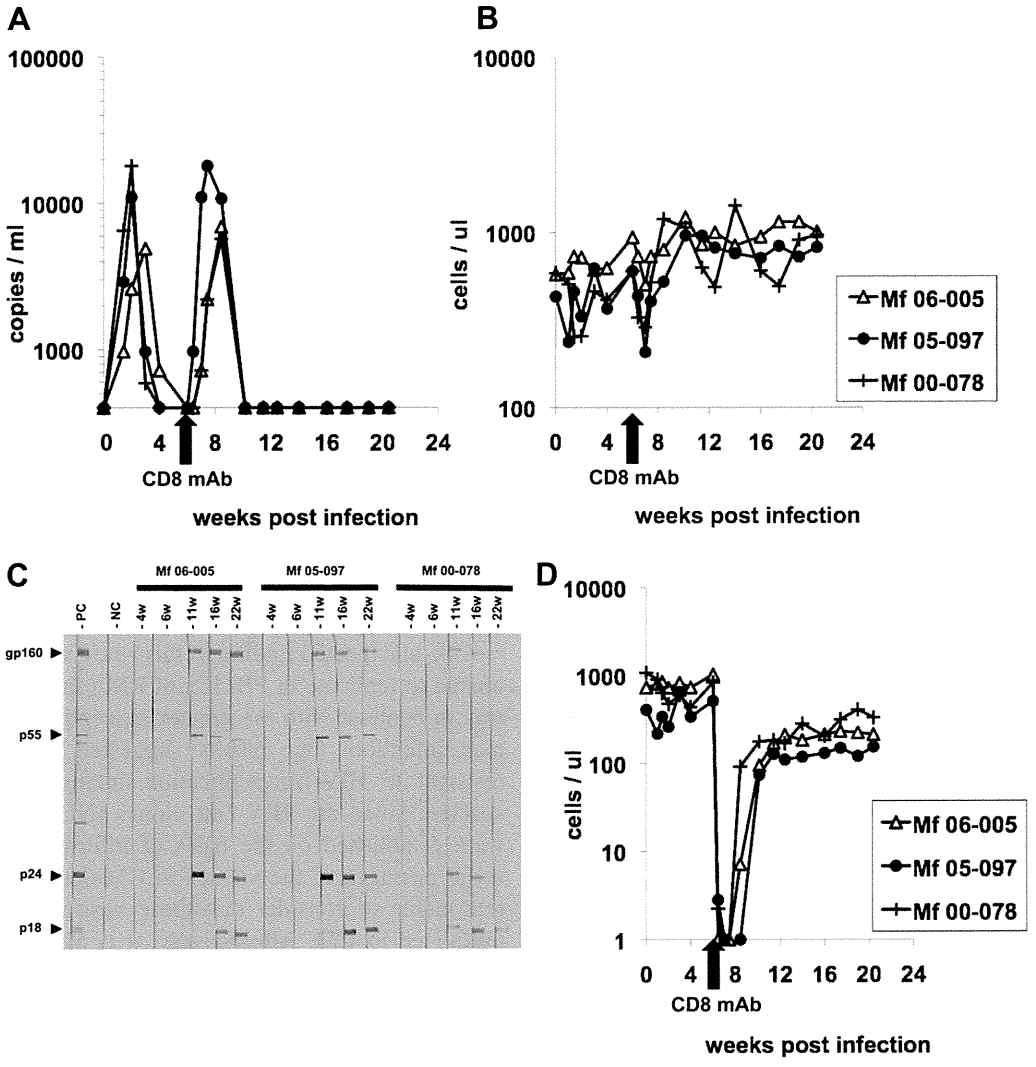

Fig. 6. Profiles of plasma viral RNA loads (A), circulating $CD4^+$ T lymphocytes (B), anti-HIV-1 antibody responses (C) and circulating $CD8^+$ T lymphocytes (D) in CM infected with HIV-1 derivatives. Viral stocks for inoculation were prepared in $CD8^+$ cell-depleted PBMCs and then 10 ng of p24 of HIV-1 were inoculated into each animal. Commercially available diagnostic HIV-1 Western blotting strips were reacted with 100-fold diluted plasma of each monkey. Plasma from HIV-1 infected or uninfected individuals was used as a positive or negative control, respectively. The black arrow indicates the day of anti-CD8 mAb (cM-T807) inoculation.

We demonstrated that the reappearance of viremia was observed in all monkeys tested in parallel with decline of $CD8^+$ T cells after anti-CD8 mAb administration (Fig. 6A and D). This result indicated that HIV-1-specific $CD8^+$ T cells had a critical role in the control of HIV-1mt replication and suggested that the virus may be able to infect latently in vivo. In order to establish a set point viremia and persistent infection, further modifications of HIV-1mt may be required to enable potent escape from the anti-viral immune response.

Further mechanistic characterization of anti-HIV-1 restriction factors will help in the construction of highly replicative and pathogenic HIV-1mt clones. As in the case of SHIV, in vivo passage of the virus could be a conventional and straightforward procedure for achieving such purposes [4]. However, the results of our study demonstrate that selective modification of HIV-1mt based on available knowledge regarding the molecular machineries is an alternative and powerful way. We are now in the process of developing the next generation of HIV-1mt that will acquire growth ability and pathogenicity in macaques as well as in humans.

Acknowledgements

The authors wish to thank T. Kurosawa, M. Fujita and M. Yasue for their helpful assistance. The authors also thank F. Ono, Y. Katakai, K. Komatsuzaki, A. Hiyaoka, K. Ohto, H. Ohto, and Y. Emoto for their support in animal experiments. We also thank M. Kaizu for his technical support. The anti-CD8 antibody used in the present study was provided by the NIH Nonhuman Primate Reagent Resource (R24 RR016001, N01 AI040101). This work was supported by grants from the Japan Health Sciences Foundation and the Ministry of Health, Labor, and Welfare in Japan and by Global COE Program A06 of Kyoto University.

References

[1] N.L. Letvin, M.D. Daniel, P.K. Sehgal, R.C. Desrosiers, R.D. Hunt, L.M. Waldron, J.J. MacKey, D.K. Schmidt, L.V. Chalifoux, N.W. King, Induction of AIDS-like disease in macaque monkeys with T-cell tropic retrovirus STLV-III, Science 230 (1985) 71–73.

[2] H. Kestler, T. Kodama, D. Ringler, M. Marthas, N. Pedersen, A. Lackner, D. Regier, P. Sehgal, M. Daniel, N. King, et al., Induction of AIDS in rhesus monkeys by molecularly cloned simian immunodeficiency virus, Science 248 (1990) 1109–1112.

[3] R. Shibata, M. Kawamura, H. Sakai, M. Hayami, A. Ishimoto, A. Adachi, Generation of a chimeric human and simian immunodeficiency virus infectious to monkey peripheral blood mononuclear cells, J. Virol. 65 (1991) 3514–3520.

[4] K.A. Reimann, J.T. Li, R. Veazey, M. Halloran, I.W. Park, G.B. Karlsson, J. Sodroski, N.L. Letvin, A chimeric simian/human immunodeficiency virus expressing a primary patient human immunodeficiency virus type 1 isolate env causes an AIDS-like disease after in vivo passage in rhesus monkeys, J. Virol. 70 (1996) 6922–6928.

[5] M. Nomaguchi, N. Doi, K. Kamada, A. Adachi, Species barrier of HIV-1 and its jumping by virus engineering, Rev. Med. Virol. 18 (2008) 261–275.

[6] D. Sauter, A. Specht, F. Kirchhoff, Tetherin: holding on and letting go, Cell 141 (2010) 392–398.

[7] M. Stremlau, C.M. Owens, M.J. Perron, M. Kiessling, P. Autissier, J. Sodroski, The cytoplasmic body component TRIM5alpha restricts HIV-1 infection in Old World monkeys, Nature 427 (2004) 848–853.

[8] E.E. Nakayama, T. Shioda, Anti-retroviral activity of TRIM5 alpha, Rev. Med. Virol. 20 (2010) 77–92.

[9] A.M. Sheehy, N.C. Gaddis, J.D. Choi, M.H. Malim, Isolation of a human gene that inhibits HIV-1 infection and is suppressed by the viral Vif protein, Nature 418 (2002) 646–650.

[10] S. Henriet, G. Mercenne, S. Bernacchi, J.C. Paillart, R. Marquet, Tumultuous relationship between the human immunodeficiency virus type 1 viral infectivity factor (Vif) and the human APOBEC-3G and APOBEC-3F restriction factors, Microbiol. Mol. Biol. Rev. 73 (2009) 211–232.

[11] M.H. Malim, APOBEC proteins and intrinsic resistance to HIV-1 infection, Philos. Trans. R Soc. Lond B. Biol. Sci. 364 (2009) 675–687.

[12] S.J. Neil, T. Zang, P.D. Bieniasz, Tetherin inhibits retrovirus release and is antagonized by HIV-1 Vpu, Nature 451 (2008) 425–430.

[13] J.L. Douglas, J.K. Gustin, K. Viswanathan, M. Mansouri, A.V. Moses, K. Fruh, The great escape: viral strategies to counter BST-2/tetherin, PLoS Pathog. 6 (2010) e1000913.

[14] R. Mariani, D. Chen, B. Schrofelbauer, F. Navarro, R. Konig, B. Bollman, C. Munk, H. Nymark-McMahon, N.R. Landau, Species-specific exclusion of APOBEC3G from HIV-1 virions by Vif, Cell 114 (2003) 21–31.

[15] B. Jia, R. Serra-Moreno, W. Neidermyer, A. Rahmberg, J. Mackey, I.B. Fofana, W.E. Johnson, S. Westmoreland, D.T. Evans, Species-specific activity of SIV Nef and HIV-1 Vpu in overcoming restriction by tetherin/BST2, PLoS Pathog. 5 (2009) e1000429.

[16] K. Kamada, T. Igarashi, M.A. Martin, B. Khamsri, K. Hatcho, T. Yamashita, M. Fujita, T. Uchiyama, A. Adachi, Generation of HIV-1 derivatives that productively infect macaque monkey lymphoid cells, Proc Natl Acad Sci U S A 103 (2006) 16959–16964.

[17] T. Igarashi, R. Iyengar, R.A. Byrum, A. Buckler-White, R.L. Dewar, C. E. Buckler, H.C. Lane, K. Kamada, A. Adachi, M.A. Martin, Human immunodeficiency virus type 1 derivative with 7% simian immunodeficiency virus genetic content is able to establish infections in pig-tailed macaques, J. Virol. 81 (2007) 11549–11552.

[18] A. Kuroishi, A. Saito, Y. Shingai, T. Shioda, M. Nomaguchi, A. Adachi, H. Akari, E.E. Nakayama, Modification of a loop sequence between alpha-helices 6 and 7 of virus capsid (CA) protein in a human immunodeficiency virus type 1 (HIV-1) derivative that has simian immunodeficiency virus (SIVmac239) vif and CA alpha-helices 4 and 5 loop improves replication in cynomolgus monkey cells, Retrovirology 6 (2009) 70.

[19] A. Adachi, H.E. Gendelman, S. Koenig, T. Folks, R. Willey, A. Rabson, M.A. Martin, Production of acquired immunodeficiency syndrome-associated retrovirus in human and nonhuman cells transfected with an infectious molecular clone, J. Virol. 59 (1986) 284–291.

[20] T. Yamashita, N. Doi, A. Adachi, M. Nomaguchi, Growth ability in simian cells of monkey cell-tropic HIV-1 is greatly affected by downstream region of the vif gene, J. Med. Invest. 55 (2008) 236–240.

[21] H. Akari, K.H. Nam, K. Mori, I. Otani, H. Shibata, A. Adachi, K. Terao, Y. Yoshikawa, Effects of SIVmac infection on peripheral blood CD4+CD8+ T lymphocytes in cynomolgus macaques, Clin. Immunol. 91 (1999) 321–329.

[22] R.L. Willey, D.H. Smith, L.A. Lasky, T.S. Theodore, P.L. Earl, B. Moss, D.J. Capon, M.A. Martin, In vitro mutagenesis identifies a region within the envelope gene of the human immunodeficiency virus that is critical for infectivity, J. Virol. 62 (1988) 139–147.

[23] J.E. Schmitz, M.A. Simon, M.J. Kuroda, M.A. Lifton, M.W. Ollert, C.W. Vogel, P. Racz, K. Tenner-Racz, B.J. Scallon, M. Dalesandro, J. Ghrayeb, E.P. Rieber, V.G. Sasseville, K.A. Reimann, A nonhuman primate model for the selective elimination of CD8+ lymphocytes using a mouse-human chimeric monoclonal antibody, Am. J. Pathol. 154 (1999) 1923–1932.

[24] C.A. Virgen, Z. Kratovac, P.D. Bieniasz, T. Hatziioannou, Independent genesis of chimeric TRIM5-cyclophilin proteins in two primate species, Proc. Natl. Acad. Sci. U S A 105 (2008) 3563–3568.

Arch Virol
DOI 10.1007/s00705-011-1178-6

BRIEF REPORT

$CD16^+$ natural killer cells play a limited role against primary dengue virus infection in tamarins

Tomoyuki Yoshida · Tsutomu Omatsu · Akatsuki Saito · Yuko Katakai · Yuki Iwasaki · Sayuki Iijima · Terue Kurosawa · Masataka Hamano · Shinichiro Nakamura · Tomohiko Takasaki · Yasuhiro Yasutomi · Ichiro Kurane · Hirofumi Akari

Received: 29 July 2011 / Accepted: 12 November 2011

Abstract CD16 is a major molecule expressed on NK cells. To directly assess the role of natural killer (NK) cells in dengue virus (DENV) infection *in vivo*, CD16 antibody-treated tamarins were inoculated with a DENV-2 strain. This resulted in the transient depletion of $CD16^+$ NK cells, whereas no significant effects on the overall levels or kinetics of plasma viral loads and antiviral antibodies were observed in the treated monkeys when compared to control monkeys. It remains elusive whether the $CD16^-$ NK subpopulation could play an important role in the control of primary DENV infection.

Keywords Dengue virus · Tamarin · NK cells · CD16

T. Yoshida and T. Omatsu contributed equally to this study.

Electronic supplementary material The online version of this article (doi:10.1007/s00705-011-1178-6) contains supplementary material, which is available to authorized users.

T. Yoshida · Y. Iwasaki · S. Iijima · T. Kurosawa · M. Hamano · Y. Yasutomi · H. Akari
Tsukuba Primate Research Center, National Institute of Biomedical Innovation, 1-1 Hachimandai, Tsukuba, Ibaraki 305-0843, Japan

T. Yoshida (✉) · A. Saito · H. Akari (✉)
Center for Human Evolution Modeling Research, Primate Research Institute, Kyoto University, Inuyama, Aichi 484-8506, Japan
e-mail: ytomoyuki@pri.kyoto-u.ac.jp

H. Akari
e-mail: akari@pri.kyoto-u.ac.jp

T. Omatsu · T. Takasaki · I. Kurane
Department of Virology I, National Institute of Infectious diseases, 1-23-1 Toyama, Shinjuku-ku, Tokyo 162-8640, Japan

DENV is one of the most serious mosquito-borne virus affecting humans, with 2.5 billion people at risk in tropical and subtropical regions around the world each year [12]. A wide variety of clinical manifestations have been noted, which range from asymptomatic, mild febrile illness (dengue fever [DF]) to dengue hemorrhagic fever (DHF)/dengue shock syndrome (DSS), a life-threatening illness. It has been shown that humans with a secondary heterologous DENV infection are at a higher risk of contracting severe dengue disease [10, 26]. DHF/DSS occurs in infants during primary DENV infection, predominantly in the second half of the first year of life, when maternal antibodies have low residual neutralizing activity [11, 17].

NK cells are a component of the innate immune system that plays a central role in host defense against viral infection and tumor cells. It has been shown that infection by some viruses, such as herpes simplex virus-1, influenza virus or ectromelia poxvirus, can be controlled by NK cells in mice [15]. Yet the most compelling evidence for a role

A. Saito
International Research Center for Infectious Diseases, The Institute of Medical Science, The University of Tokyo, 4-6-1 Shirokanedai, Minato-ku, Tokyo 108-8639, Japan

Y. Katakai
Corporation for Production and Research of Laboratory Primates, 1-1 Hachimandai, Tsukuba, Ibaraki 305-0843, Japan

S. Nakamura
Research Center for Animal Life Science, Shiga University of Medical Science, Seta Tsukinowa-cho, Otsu, Shiga 520-2192, Japan

Published online: 03 December 2011

of NK cells in early defense against viruses was obtained in a study showing increased susceptibility to murine cytomegalovirus (MCMV) after NK cell depletion and increased resistance after adoptive transfer of NK cells [23]. Defects in NK cell activity, such as decreased production of interferon (IFN)-γ or cytotoxicity, render mice more susceptible to MCMV infection [23]. NK cells can kill virus-infected cells by using cytotoxic granules or by recognizing and inducing lysis of antibody-coated target cells (antibody-dependent cell cytotoxicity) via an Fc-binding receptor such as CD16 [21].

Early activity of NK cells may be important for clearing primary DENV infection [24]. In a DENV mouse model, mice experimentally infected with DENV showed increased NK cell levels [24]. A significant increase in the frequency of NK cell circulation was also shown in patients who developed an acute dengue disease [2]. In addition, patients with a mild dengue disease have elevated NK cell rates when compared to those with severe dengue diseases [9, 27]. Moreover, Kurane *et al.* [14] reported that human blood NK cells are cytotoxic against DENV-infected cells in target organs via direct cytolysis and antibody-dependent cell-mediated cytotoxicity. It was also shown that the intracellular cytotoxic granule, TIA-1, was up-regulated early in NK cells in the acute phase of DENV infection and that NK-activating receptor NKp44 was involved in virus-mediated NK activation through direct interaction with DENV envelope protein [2, 13]. These results suggest that the early activation of NK cells contributes to the prevention of the severe dengue disease. However, based on quantitative and functional analyses in animal models *in vivo*, defining the contribution of NK cells to suppression of DENV replication *in vivo* has been necessary.

We have recently reported that common marmosets (*Callithrix jacchus*) are highly permissive to DENV infection [22]. These New World monkeys, being nonhuman primates, are considered to have an immune system similar to that of humans [28, 29]. The present study was initiated to investigate the role of NK cells in controlling DENV during primary infection in our nonhuman primate model.

The animals were cared for in accordance with National Institute of Biomedical Innovation rules and guidelines for experimental animal welfare, and all protocols were approved by our Institutional Animal Study Committee. Eight tamarins (*Saguinus midas* and *Saguinus labiatus*) were used in this study. As marmosets and tamarins are closely related monkey species and are classified as members of the Callitrichinae, we expected that tamarins would also be permissive to DENV infection, like marmosets. To check the permissiveness of tamarins to DENV, 2 tamarins were infected with DENV-2 (DHF0663 strain: 6.7×10^7 PFU/ml) subcutaneously or intravenously (Fig. 1).

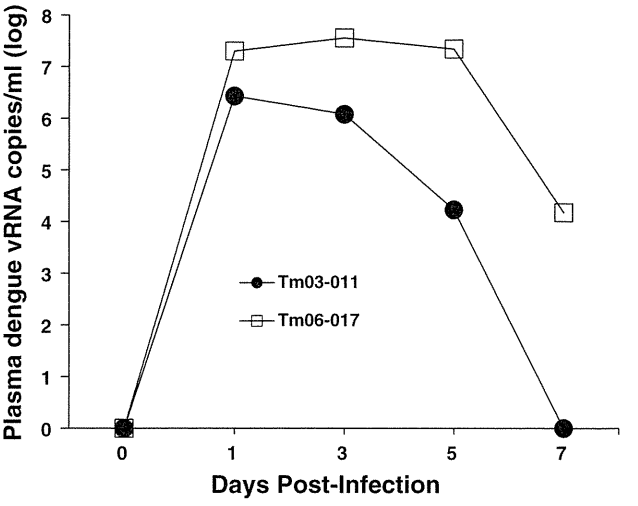

Fig. 1 Levels of vRNA in DENV-infected tamarins. Tamarins were infected subcutaneously or intravenously with DENV at a dose of 6.7×10^7 PFU/ml. The vRNAs were detected in plasma by real-time PCR. Tm03-011, subcutaneous infection; Tm06-017, intravenous infection

Dengue viral RNA (vRNA), which was quantified using real-time PCR as previously described [22], was detected in plasma samples from the tamarins on day 1 post-infection. For each of the two tamarins (Tm03-011, Tm06-017), the plasma vRNA levels reached 2.7×10^6 copies/ml and 2.0×10^7 copies/ml on day 1 post-infection, respectively, and were detectable on days 3 and 5. These results indicate that tamarins are also permissive to DENV infection, which is consistent with the results obtained by using marmosets [22].

Next, we sought to assess the role of NK cells in DENV infection *in vivo*. In this regard, in vivo depletion of NK cells by the administration of NK-specific monoclonal antibody (mAb) was considered to be straightforward to directly address the question. We employed a new method by which an anti-CD16 mAb 3G8 [7] but not a control mAb MOPC-21 efficiently depleted a major NK population expressing CD16 in tamarins, as we recently reported [29]. The mouse anti-human CD16 mAb 3G8 was produced in serum-free medium and purified using protein A affinity chromatography. Endotoxin levels were confirmed to be lower than 1 EU/mg. Four red-handed tamarins and two white-lipped tamarins (*Saguinus labiatus*) were used in this experiment. Three tamarins were intravenously administered 3G8 at a dose of 50 mg/kg, while others were given a control mAb MOPC-21. One day later, both mAb-treated tamarins were subcutaneously inoculated with 3×10^5 PFU/ml of DENV-2 DHF0663 strain on the basis of a previous report that a single mosquito might inject between 10^4 and 10^5 PFU of DENV into a human [20]. It was confirmed that at 1-3 days after the 3G8 mAb treatment, $CD16^+$ cells were almost completely depleted in the

tamarins followed by recovery to the initial levels at around 2 weeks after administration, while the cells were maintained at the initial levels in the monkeys with MOPC-21 (Fig. 2a). In addition, it is noteworthy that the ratios of CD4$^+$ and CD8$^+$ T cells and CD20$^+$ B cells were not affected by the administration of the 3G8 mAb (Supplementary Figure 1). In the case of administration of mAb MOPC-21, we confirmed no significant effect on CD16$^+$ cells (Supplementary Figure 2). The killing activities of the peripheral blood mononuclear cells (PBMCs) taken from the 3G8-treated monkeys were reduced at day 1 post-antibody-treatment, followed by an increase irrespective of depletion of CD16$^+$ NK cells at day 2 post-antibody-treatment (1 day after DENV inoculation), suggesting that the CD16$^-$ NK population may be activated by DENV infection (Fig. 2b). Plasma viral loads in both mAb-treated monkeys rose to 10^5 copies/ml by day 1 after infection and then reached a peak at 10^6 copies/ml on day 3 or day 7, followed by a rapid decline, with values dipping below the detectable level by day 14 after infection (Fig. 2c). These results suggested that CD16$^+$ NK cells apparently did not contribute to DENV replication in the acute phase in our tamarin model.

It was reported previously that non-structural glycoprotein NS1 is essential for flavivirus viability and that the NS1 protein circulates during the acute phase of disease in the plasma of patients infected with DENV [1]. Epidemiological studies have demonstrated that secreted NS1 levels are correlated with viremia levels and are higher in cases of DHF than in dengue fever (DF) early in illness [16]. Thus, it has been suggested that NS1 might be a useful marker as an indicator of the severity of dengue disease. We have used the level of the NS1 antigen as an alternative diagnostic marker to examine the effects of CD16 antibody treatment on DENV replication. The NS1 was measured by Platelia Dengue NS1 Ag assay (BioRad). Antigenemia was observed in these infected monkeys between 3-14 days post-infection. Serum IgM and IgG specific for DENV antigens were measured by ELISA. DENV-specific IgM or IgG antibody was equally detected in both mAb-treated monkeys (Fig. 3).

We recently demonstrated that marmosets are permissive to DENV infection [22]. In this study, we found that tamarins are also permissive to DENV infection (Fig. 1). Moreover, we also investigated the role of NK cells against early DENV infection using *in vivo* depletion of CD16$^+$

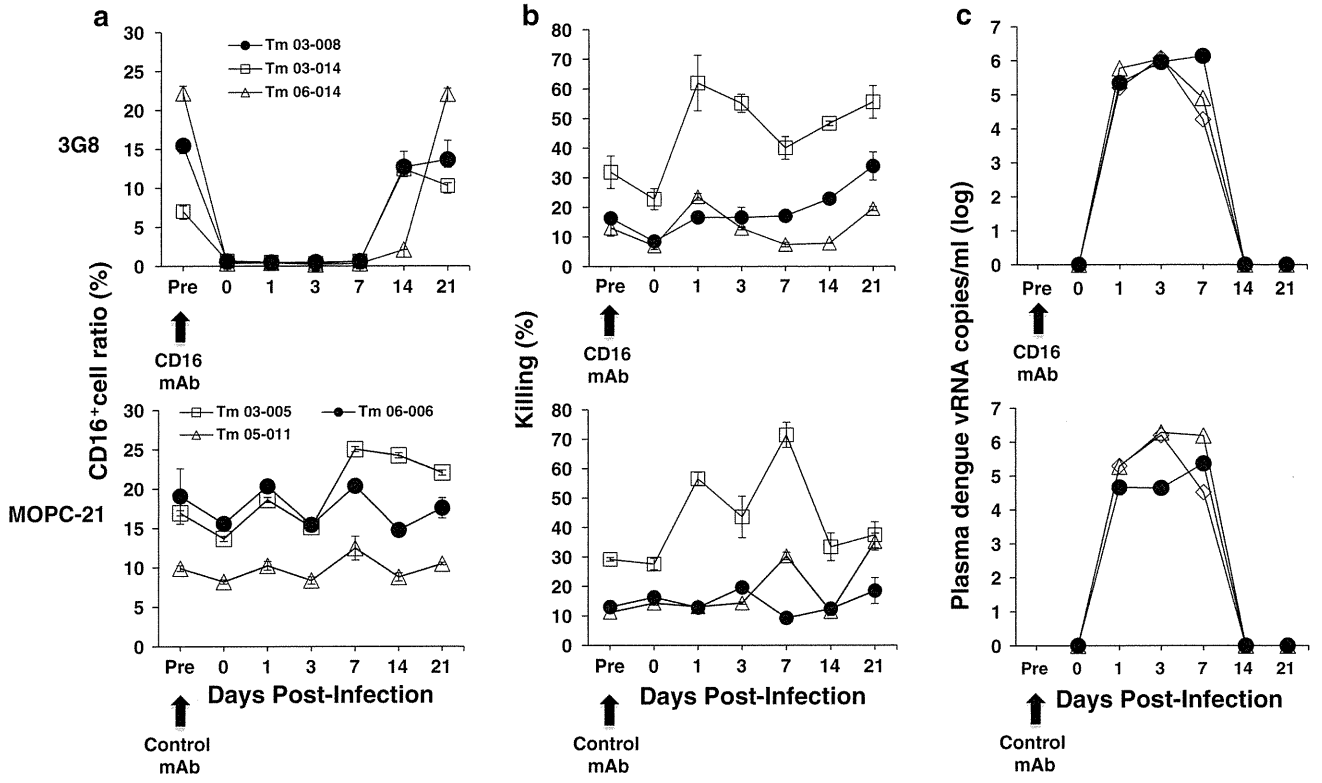

Fig. 2 Ratios of CD16$^+$ NK cells, killing activity of PBMCs, and vRNA in DENV-infected tamarins after treatment with 3G8 or MOPC-21 mAb. Tamarins were infected subcutaneously with DENV at a dose $3x10^5$ PFU/ml after treatment with 50 mg/kg of 3G8 or MOPC-21 mAb. **a** Ratios of CD16$^+$ NK cells were determined in whole-blood specimens. **b** The activities of NK cells were determined in PBMCs of tamarins by NK cytotoxic assay. **c** The vRNAs were detected in plasma by real-time PCR

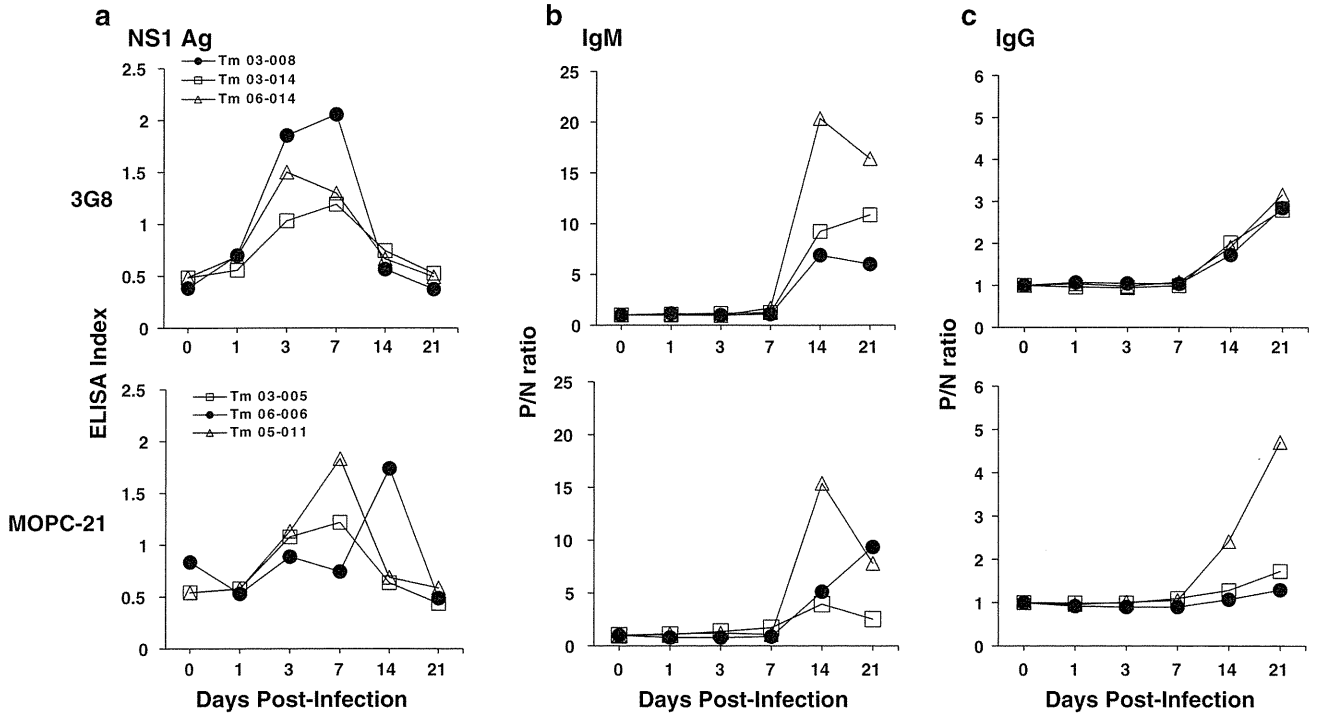

Fig. 3 Levels of NS1 antigen and DENV-specific IgM and IgG in plasma samples from DENV-infected tamarins after treatment with 3G8 or MOPC-21 mAb. The levels of NS1 antigen and DENV-specific IgM and IgG in plasma were measured by ELISA. **a** ELISA index of NS1 antigen, **b** positive/negative (P/N) ratio of DENV-specific IgM, **c** P/N ratio of DENV-specific IgG in plasma samples from DENV-infected tamarins after administration of the 3G8 or MOPC-21 mAb. The P/N ratio was calculated as the optical density of the test sample divided by that of a negative sample. P/N ratios <2 and ≥2 were considered to be negative and positive, respectively. Top, 3G8; bottom, MOPC-21 mAb

NK cells in tamarins and found that the depletion of $CD16^+$ NK cells had almost no effect on DENV replication (Fig. 2), indicating that this NK subpopulation is unlikely to contribute to controlling DENV replication. Interestingly, these results imply that the $CD16^-$ NK subpopulation may have a critical role of controlling DENV infection *in vivo*.

Using our model, we investigated the role of NK cells *in vivo* against DENV infection, which remains to be elucidated in several aspects. We previously reported that almost complete *in vivo* depletion of the $CD16^+$ NK subpopulation was not able to completely remove the NK-mediated cytotoxic activity in tamarins [29]. In this study, despite a transient but substantial reduction in the $CD16^+$ NK cell number following 3G8 treatment in tamarins, DENV replication was comparable to that in monkeys that received the control mAb. The NK-mediated cytotoxic activity was augmented in both study groups, indicating that $CD16^-$ NK cells were responsible for the cytotoxic activity and suggesting that they might play a role in controlling DENV replication.

The next question is how $CD16^-$ NK cells may regulate DENV infection. One possibility regarding $CD16^-$ NK cells is that $CD56^+$ or $CD57^+$ NK cells are involved in controlling DENV infection. Human NK cells are classically divided into two functional subsets based on their cell-surface density of CD56 and CD16, i.e., $CD56^{bright}CD16^-$ immunoregulatory cells and $CD56^{dim}CD16^+$ cytotoxic cells. Both subsets have been characterized extensively regarding their different functions, phenotypes, and tissue localization [8]. The NK cell number is maintained by a continuous differentiation process associated with the expression of CD57 that results in NK cells with poor responsiveness to cytokine stimulation but high cytolytic capacity [3, 18]. The second possibility is that $CD16^-$ NK cells have a non-cytolytic helper function. Generally, it is well known that NK cells possess both a cytolytic and a non-cytolytic helper function. It has been suggested that cytokine production is carried out by $CD56^{bright}CD16^-$ NK cells [4–6]. Interferon (IFN)-γ secreted by NK cells has shown potent antiviral effects against DENV infection in early phases [25]. One aspect of the NK helper function arises from recent evidence indicating that NK cells can be induced to function as non-cytotoxic helper cells following stimulation with interleukin-18 [19]. This cytokine induces IFN-γ secretion from NK cells and thus enables dendritic cells (DCs) to secrete IL-12, leading to Th1 polarization [19]. It is possible that $CD16^-$ NK cells, which have poor

cytotoxic activity but an enhanced ability to secrete cytokines and then lead to a Th1 response, are preserved during 3G8 administration. The persistence of this minor CD16$^-$ NK cell subpopulation could exert an antiviral effect through INF-γ-mediated pathways despite the depletion of CD16$^+$ NK cells. The third possibility is that CD16$^+$ NK cells of tamarins play pivotal roles against bacterial infections and cancer progression but not DENV-infected cells. We will address these possibilities for the roles of the NK subpopulation in the future studies.

In conclusion, this study provides a DENV *in vivo* replication model in tamarins and new information on the possible role of CD16$^+$ NK cells in DENV replication *in vivo*. It remains elusive whether the CD16$^+$ and CD16$^-$ NK subpopulations could play an important role in the control of primary DENV infection.

Acknowledgments We would like to give special thanks to members of the Corporation for Production and Research of Laboratory Primates for technical assistance. We also would like to give special thanks to Ms. Tomoko Ikoma and Ms. Mizuho Fujita for technical assistance. Moreover, we appreciate Dr. Keith A. Reimann (the NIH Nonhuman Primate Reagent Resource R24 RR016001, NIAID contact HHSN272200900037C) for providing CD16 antibody. This work was supported by grants from the Ministry of Health, Labor and Welfare of Japan (to Hirofumi Akari and Ichiro Kurane). This research was also supported by the Environment Research and Technology Development Fund (D-1007) from the Ministry of the Environment of Japan (to Tomoyuki Yoshida and Hirofumi Akari).

Conflict of interest The authors declare that the research was conducted in the absence of any commercial or financial relationships that could be construed as a potential conflict of interest.

References

1. Alcon-LePoder S, Sivard P, Drouet MT, Talarmin A, Rice C, Flamand M (2006) Secretion of flaviviral non-structural protein NS1: from diagnosis to pathogenesis. Novartis Found Symp 277:233–247 (discussion 247–253)
2. Azeredo EL, De Oliveira-Pinto LM, Zagne SM, Cerqueira DI, Nogueira RM, Kubelka CF (2006) NK cells, displaying early activation, cytotoxicity and adhesion molecules, are associated with mild dengue disease. Clin Exp Immunol 143:345–356
3. Bjorkstrom NK, Riese P, Heuts F, Andersson S, Fauriat C, Ivarsson MA, Bjorklund AT, Flodstrom-Tullberg M, Michaelsson J, Rottenberg ME, Guzman CA, Ljunggren HG, Malmberg KJ (2010) Expression patterns of NKG2A, KIR, and CD57 define a process of CD56dim NK-cell differentiation uncoupled from NK-cell education. Blood 116:3853–3864
4. Caligiuri MA (2008) Human natural killer cells. Blood 112: 461–469
5. Cooper MA, Fehniger TA, Turner SC, Chen KS, Ghaheri BA, Ghayur T, Carson WE, Caligiuri MA (2001) Human natural killer cells: a unique innate immunoregulatory role for the CD56(bright) subset. Blood 97:3146–3151
6. Farag SS, Caligiuri MA (2006) Human natural killer cell development and biology. Blood Rev 20:123–137
7. Fleit HB, Wright SD, Unkeless JC (1982) Human neutrophil Fc gamma receptor distribution and structure. Proc Natl Acad Sci USA 79:3275–3279
8. Gayoso I, Sanchez-Correa B, Campos C, Alonso C, Pera A, Casado JG, Morgado S, Tarazona R, Solana R (2011) Immunosenescence of human natural killer cells. J Innate Immun 3:337–343
9. Green S, Pichyangkul S, Vaughn DW, Kalayanarooj S, Nimmannitya S, Nisalak A, Kurane I, Rothman AL, Ennis FA (1999) Early CD69 expression on peripheral blood lymphocytes from children with dengue hemorrhagic fever. J Infect Dis 180:1429–1435
10. Guzman MG, Kouri G, Valdes L, Bravo J, Alvarez M, Vazques S, Delgado I, Halstead SB (2000) Epidemiologic studies on Dengue in Santiago de Cuba, 1997. Am J Epidemiol 152: 793–799 (discussion 804)
11. Halstead SB, Lan NT, Myint TT, Shwe TN, Nisalak A, Kalyanarooj S, Nimmannitya S, Soegijanto S, Vaughn DW, Endy TP (2002) Dengue hemorrhagic fever in infants: research opportunities ignored. Emerg Infect Dis 8:1474–1479
12. Halstead SB (2007) Dengue. Lancet 370:1644–1652
13. Hershkovitz O, Rosental B, Rosenberg LA, Navarro-Sanchez ME, Jivov S, Zilka A, Gershoni-Yahalom O, Brient-Litzler E, Bedouelle H, Ho JW, Campbell KS, Rager-Zisman B, Despres P, Porgador A (2009) NKp44 receptor mediates interaction of the envelope glycoproteins from the West Nile and dengue viruses with NK cells. J Immunol 183:2610–2621
14. Kurane I, Hebblewaite D, Ennis FA (1986) Characterization with monoclonal antibodies of human lymphocytes active in natural killing and antibody-dependent cell-mediated cytotoxicity of dengue virus-infected cells. Immunology 58:429–436
15. Lee SH, Miyagi T, Biron CA (2007) Keeping NK cells in highly regulated antiviral warfare. Trends Immunol 28:252–259
16. Libraty DH, Young PR, Pickering D, Endy TP, Kalayanarooj S, Green S, Vaughn DW, Nisalak A, Ennis FA, Rothman AL (2002) High circulating levels of the dengue virus nonstructural protein NS1 early in dengue illness correlate with the development of dengue hemorrhagic fever. J Infect Dis 186:1165–1168
17. Libraty DH, Acosta LP, Tallo V, Segubre-Mercado E, Bautista A, Potts JA, Jarman RG, Yoon IK, Gibbons RV, Brion JD, Capeding RZ (2009) A prospective nested case-control study of Dengue in infants: rethinking and refining the antibody-dependent enhancement dengue hemorrhagic fever model. PLoS Med 6:e1000171
18. Lopez-Verges S, Milush JM, Pandey S, York VA, Arakawa-Hoyt J, Pircher H, Norris PJ, Nixon DF, Lanier LL (2010) CD57 defines a functionally distinct population of mature NK cells in the human CD56dimCD16+ NK-cell subset. Blood 116:3865–3874
19. Mailliard RB, Alber SM, Shen H, Watkins SC, Kirkwood JM, Herberman RB, Kalinski P (2005) IL-18-induced CD83+CCR7+ NK helper cells. J Exp Med 202:941–953
20. Mathew A, Rothman AL (2008) Understanding the contribution of cellular immunity to dengue disease pathogenesis. Immunol Rev 225:300–313
21. Navarro-Sanchez E, Despres P, Cedillo-Barron L (2005) Innate immune responses to dengue virus. Arch Med Res 36:425–435
22. Omatsu T, Moi ML, Hirayama T, Takasaki T, Nakamura S, Tajima S, Ito M, Yoshida T, Saito A, Katakai Y, Akari H, Kurane I (2011) Common marmoset (Callithrix jacchus) as a primate model of dengue virus infection: development of high levels of viremia and demonstration of protective immunity. J Gen Virol 92:2271–2280. doi:10.1099/vir.0.031229-0
23. Scalzo AA, Corbett AJ, Rawlinson WD, Scott GM, Degli-Esposti MA (2007) The interplay between host and viral factors in shaping the outcome of cytomegalovirus infection. Immunol Cell Biol 85:46–54
24. Shresta S, Kyle JL, Robert Beatty P, Harris E (2004) Early activation of natural killer and B cells in response to primary dengue virus infection in A/J mice. Virology 319:262–273